NUMERICAL SOLUTIONS OF ORDINARY DIFFERENTIAL EQUATIONS USING ELEMENT FREE GALERKIN METHOD

Thesis Submitted in partial fulfillment of the requirements for

The award of degree of

Masters of Science

In

Mathematics and Computing

Submitted by

Harpreet Kaur

Reg. No.-301303003

Under

the guidance of

Dr. Vivek Sangwan

and

Dr. Rajesh Kumar Sharma

School of Mathematics

Thapar University, Patiala-147004

PUNJAB, INDIA

July, 2015

CERTIFICATE

I hereby certify that the work which is being presented in the thesis entitled **"NUMERICAL SOLUTIONS OF ORDINARY DIFFERENTIAL EQUATIONS USING ELEMENT FREE GALERKIN METHOD"** in partial fulfillment of the requirements for the award of degree of Master of Science in "Mathematics and Computing" to the School of Mathematics, Thapar University, Patiala is an authentic record of my own work studied under the supervision of Dr. Vivek Sangwan and Dr. Rajesh Kumar Sharma.

The matter presented in this thesis has not been submitted for the award of any other degree of this or any other university.

Harpreet Kaur

(*Harpreet Kaur*)

Reg. No. 301303003

This is to certify that the above statement made by the candidate is correct and true to the best of my knowledge.

Dr. Rajesh Kumar Sharma
Assistant Professor
Dept. of Mathematics
NIT Jaipur

V. Sangwan

Dr. Vivek Sangwan
Assistant Professor
School of Mathematics
Thapar University, Patiala

Countersigned by:

Dr. A.K. Lal
Professor and Head, SOM
Thapar University, Patiala.

Dr. S.S. Bhatia
Dean of Academic Affairs
Thapar University, Patiala.

ACKNOWLEDGEMENTS

I would like to thank my supervisor, **Dr. Vivek Sangwan**, Assistant Professor, School of Mathematics, Thapar University, Patiala, and **Dr. Rajesh Kumar Sharma**, Assistant Professor, Dept. of Mathematics, NIT Jaipur, for the patient guidance, encouragement and advice he has provided throughout my time as his student. I have been extremely lucky to have a supervisor who cared so much about my work, and who responded to my questions and queries so promptly.

I would like to express my sincere thanks to **Dr. A.K. Lal**, Head SOM, Thapar University, Patiala, for providing the necessary facilities needed for this work and directly or indirectly encouraged me to do work. I would also thank all academic and administrative staff of School of Mathematics, Thapar University, Patiala who have contributed directly or indirectly to this work.

I would also like to thank my mother for their continuous support which inspired me and encouraged me, without them I would not be able to complete my work.

Life at Thapar University, Patiala has been enjoyable with friends who have been always there for me, listening to me, rejoicing me, complaining and pondering my way throughout my study. I thank them all for their great company and finally to God who made all the things possible.

(HARPREET KAUR)

ABSTRACT

Differential equations play an important role in almost all areas of science and engineering, for example physics, economics, biology, fluid dynamics, fluid mechanics, aerodynamics, etc. But the analytic solution can not be determined for most of the differential equations governing realistic model problems using analytical techniques. Therefore, we need to depend upon the numerical methods to find the approximate solution. Finite element techniques have been widely used for solving the differential equations. But from the last two decades, element free Galerkin methods have drawn attention of the research community to solve real model problems. The element free Galerkin techniques have many benefits over finite element techniques. In the present study, elements free Galerkin methods have been applied to solve the fluid dynamics problems.

The whole work is divided into three chapters.

Chapter 1 introduces the basic concepts of differential equations and the solution methodology. Finite element technique have been elaborated with the help of an example. Also the concept behind the element free Galerkin methods and the need for the method have been discussed.

In **Chapter 2** a review of research paper entitled **"Element free Galerkin solution of radiative hydromagnetic micropolar flow saturated Darcy medium with heat transfer over a stretching sheet with Joule heating"** has been carried out. The paper has been discussed thoroughly. Apart from this, the concept of shape functions, weight functions and moving least square strategy has been presented.

Chapter 3 reviews the research paper entitled **"Numerical simulation of unsteady MHD flow and heat transfer of second grade fluid with viscous dissipation and Joule heating using element free approach"**. The paper has been discussed thoroughly.

The element free Galerkin technique based on moving least squares has been explained for solving the model problem. Numerical results have been discussed in the last. Numerical results shows that the results obtained using the element free Galerkin method are in good agreements with those listed in the literature.

In the last, references have been presented.

Contents

Chapter 1

Differential Equations - An Overview

1.1 Introduction

A differential equation is an equation that relates some function with its derivatives. In applications, the functions usually represent physical quantities, the derivatives represent their rates of change, and the equation defines a relationship between the two. Because such relations are extremely common, differential equations play an important role in many fields including engineering, physics, economics, biology etc. Differential equations have a remarkable ability to predict the world around us. They can describe exponential growth and decay, the population growth of species or the change in investment return over time etc. Some of the applications of the differential equations include:

1) In medicine, for modelling cancer growth or the spread of disease, etc.
2) In engineering for describing the movement of electricity, etc.
3) In chemistry for modelling chemical reactions, etc.
4) In economics to find optimum investment strategies, etc.
5) In physics to describe the motion of waves, pendulums or chaotic systems, etc.

Thus the subject of differential equation constitute a large and very important branch of modern mathematics. From the early days of calculus, the subject has been an area of great theoretical research and practical applications, and it continues to be so in the present days. Differential equations are studied from several different perspectives, mostly concerned with their solutions, the set of functions that satisfy the equation. However, only few of the differential equations are solvable for exact solutions using some specific processes or methods; though, some properties of the exact solutions of a given differential equation may be determined without finding their exact solution. Since exact solution for most of the differential equations cannot be determined, we need to take help of numerical techniques for finding approximate solution of differential equations. In the present work, we will study one of the numerical techniques, namely element free Galerkin method for solving the differential equations.

To start will we present below the definations of some concepts which are used in differential equations.

1.2 Differential equation

A relation involving derivatives of one or more dependent variables with respect to one or more independent variables is called differential equation.
For example:

$$\frac{dy}{dt} = 2y + 8.$$
$$\frac{\partial^2 u}{\partial x^2} + \frac{\partial^2 u}{\partial y^2} = 0.$$

1.3 Order of a differential equation

The order of the highest order derivatives involved in a differential equation is called the order of the differential equation.
For example:

$$y = \sqrt{x}\left(\frac{dy}{dx}\right) + \frac{k}{(\frac{dy}{dx})}, \qquad Order = 1.$$
$$\left(\frac{d^2y}{dx^2}\right)^{1/3} = \left(y + \frac{dy}{dx}\right)^{1/2}, \qquad Order = 2.$$

1.4 Degree of a differential equation

The degree of a differential equation is the degree of the highest order derivative terms which occurs in it, after the differential equation has been made free from radicals and fractions.

For example:

$$y = \sqrt{x}\left(\frac{dy}{dx}\right) + \frac{k}{(\frac{dy}{dx})}, \qquad Degree = 2.$$

$$\left(\frac{d^2y}{dx^2}\right)^{1/3} = \left(y + \frac{dy}{dx}\right)^{1/2}, \qquad Degree = 2.$$

1.5 Classification of differential equations

Differential equations are classified into two categories:

1) Ordinary differential equations

2) Partial differential equations.

1.5.1 Ordinary differential equation

A differential equation involving derivatives with respect to a single independent variable is called an ordinary differential equation [18].

For example:

$$\frac{dy}{dx} = y + sinx.$$

$$\left(\frac{d^2y}{dx^2}\right)^{1/3} = \left(y + \frac{dy}{dx}\right)^{1/2}.$$

Types of ordinary differential equations:

Ordinary differential equations can be further classified into two types:

a) Linear ordinary differential equations.

b) Nonlinear ordinary differential equations.

Linear ordinary differential equation: An ordinary differential equation is called linear if the dependent variable and every derivative involved occur in the first degree only and no product of dependent variables and/or derivatives occur.

For example:

$$\frac{dy}{dx} = x + sinx.$$
$$\frac{d^2y}{dx^2} + \frac{dy}{dx} + \frac{x}{2} = 0.$$

Nonlinear ordinary differential equation: An ordinary differential equation which is not linear is called a nonlinear ordinary differential equation.

For example:

$$y = \sqrt{x}\left(\frac{dy}{dx}\right) + \frac{k}{(\frac{dy}{dx})}.$$
$$\left(\frac{d^2y}{dx^2}\right)^{1/3} = \left(y + \frac{dy}{dx}\right)^{1/2}.$$

1.5.2 Partial differential equation

A differential equation involving derivatives with respect to more than one independent variable is called a partial differential equation.

For example:

$$\frac{\partial^2 u}{\partial x^2} + \frac{\partial^2 u}{\partial y^2} + \frac{\partial^2 u}{\partial z^2} = 0.$$
$$\frac{\partial^2 v}{\partial t^2} = k\left(\frac{\partial^3 v}{\partial x^3}\right)^2.$$

Types of partial differential equations: Partial differential equations can be classified into the following four types [18]:

a) Linear partial differential equations

b) Semilinear partial differential equations

c) Quasilinear partial differential equations

d) Nonlinear partial differential equations.

Let z be a function of two independent variables x and y.Let $p = \partial z/\partial x$ and $q = \partial z/\partial y$.

Linear partial differential equation: A partial differential equation is of linear type if can be written in the form $P(x,y)p + Q(x,y)q = R(x,y)z + S(x,y)$.

For example:

$$yx^2p + xy^2q = xyz + x^2y^3.$$

Semi-linear partial differential equation: A partial differential equation is of semi-linear type if it can be written in the form $P(x,y)p + Q(x,y)q = R(x,y,z)$.
For example:

$$xyp + x^2yq = x^2y^2z^2.$$

Quasi-linear partial differential equation: A partial differential equation is of quasi-linear type if it can be written in the form $P(x,y,z)p + Q(x,y,z)q = R(x,y,z)$.
For example:

$$x^2zp + y^2zq = xy.$$

Non-linear partial differential equation: A partial differential equation which does not come under the above three types is called non-linear differential equation.
For example:

$$p^2 + q^2 = 1.$$

1.6 Solution of differential equations

A function $f(x,y) = 0$ is said to be a solution of a given differential equation $F(x,y,y_1,y_2,...y_n) = 0$ if it satisfies the differential equation.

Solution types:

Let

$$F(x,y,y_1,y_2,...y_n) = 0 \tag{1.1}$$

be an n^{th} order ordinary differential equation.

1.6.1 General solution

A solution of (1.1) which contains n arbitrary constants is called a general solution of equation (1.1).

1.6.2 Particular solution

A solution of (1.1) obtained from general solution of (1.1) by giving some particular values to the n arbitrary constants is called a particular solution.

For example:

Let $y'' - 3y' + 2y = 0$ be any second order ordinary differential equation. Then $y = c_1e^x + c_2e^{2x}$ forms its general solution. Here c_1 and c_2 are two arbitrary constants. Therefore, particular solutions of the given differential equation are $y = e^x + e^{2x}, y = e^x - 2e^{2x}$ etc.

1.6.3 Singular solution

A solution which cannot be obtained from the general solution by giving any particular values to the arbitrary constants is called a singular solution.

For example:

Let $y'' - 2\sqrt{y} = 0$ be any ordinary differential equation. Then $y = (x + c)^2$ will be its general solution. Since $y = 0$ is also a solution of the given differential equation and it cannot be obtained from the general solution by assigning any particular value to the arbitrary constant c, hence $y = 0$ is a singular solution the differential equation.

1.7 Solution methodology

Broadly, we can categorize the solution techniques for differential equation into two categories:

1) Analytical techniques

2) Numerical techniques.

1.7.1 Analytical techniques

Using these techniques, we get exact solution of the differential equations. Some examples of analytical techniques [26] are

a) Variable separable method

b) Method of undetermined coefficients

c) Method of variation of parameters, etc.

1.7.2 Numerical techniques

Using these techniques, usually, we get approximate solution of the differential equations. Some of the numerical techniques are

a) Finite difference methods

b) Finite element methods

c) Finite volume methods

d) B-spline collocation methods

e) Element free Galerkin methods, etc.

Analytical techniques have benefits over numerical techniques in the sense that these techniques provide exact solution. But these techniques are applicable only to very restricted class of differential equations. Particularly when a differential equation is nonlinear or has complicated coefficients or when the domain of the differential equation is complex etc, in such type of cases, it becomes very difficult to apply the analytical techniques. Since most of the differential equations governing realistic model phenomenon from systems of equations or are nonlinear or have some complex coefficients etc, the analytic techniques almost fail to provide the exact solution. Numerical techniques have benefits over analytical techniques in such cases. For the present study. I will focus on one of the numerical techniques namely element free Galerkin method [13]. Firstly I will explain finite element Galerkin methods, then i will present a brief introduction to element free Galerkin method.

1.8 Finite element method

Here, I will solve a second order linear differential equation using standard Galerkin finite element method [17].

Consider a second order differential equation

$$\frac{d^2u}{dx^2} - u + x = 0 \qquad\qquad 0 \leq x \leq 1.0$$

with boundary conditions; at $x = 0, u = 1$ and

at $x = 1, \frac{du}{dx} = 1$.

Take the nodes at $x = 0, 0.2, 0.5, 0.8, 1.0$.

Therefore, we have the following elements:

$[0, 0.2], \quad [0.2, 0.5], \quad [0.5, 0.8], \quad [0.8, 1.0].$

Now, at each node x_i, we define the basis functions $\phi_i(x)$ as

$$\phi_i(x) = \begin{cases} \dfrac{x - x_{i-1}}{x_i - x_{i-1}}, & x\epsilon[x_{i-1}, x_i] \\ \dfrac{x_{i+1} - x}{x_{i+1} - x_i}, & x\epsilon[x_i, x_{i+1}] \end{cases}$$

Let the finite element approximate solution be

$$\bar{u} = \sum_{j=1}^{5} \Phi_j(x) u_j, \quad j = 1(1)5. \tag{1.2}$$

Now, the weak formulation is given by

$$\int_0^1 \left(\frac{d^2\bar{u}}{dx^2} - \bar{u} + x \right) \Phi_i(x) dx = 0, \quad i = 1(1)5. \tag{1.3}$$

Integrating by parts and using $Q = -du/dx$, we get

$$\int_0^1 \frac{d\Phi_i}{dx}\frac{d\bar{u}}{dx} dx + \int_0^1 \Phi_i(x)\bar{u} dx = \int_0^1 x\Phi_i(x) dx - \Phi_i(x_5)Q_5 + \Phi_i(x_1)Q_1. \tag{1.4}$$

Substituting the value of $\bar{u}$, equation (1.4) becomes

$$\begin{aligned} \sum_{j=1}^{5} u_j \int_0^1 \frac{d\Phi_i}{dx}\frac{d\Phi_j}{dx} dx + \sum_{j=1}^{5} u_j \int_0^1 \Phi_i(x)\Phi_j(x) dx = \int_0^1 x\Phi_i(x) dx \\ - [\Phi_i(x_5)Q_5 - \Phi_i(x_1)Q_1], i = 1(1)5. \end{aligned} \tag{1.5}$$

Integrating element wise, we get

$$\sum_{r=1}^{4}\sum_{j=1}^{5} u_j \int_{e_r} \frac{d\Phi_i}{dx}\frac{d\Phi_j}{dx} dx + \sum_{r=1}^{4}\sum_{j=1}^{5} u_j \int_{e_r} \Phi_i(x)\Phi_j(x) dx = R - T, \quad i = 1(1)5 \tag{1.6}$$

where

$$R = \sum_{r=1}^{4} \int_{e_r} x\Phi_i(x) dx \tag{1.7}$$

and

$$T = [\Phi_i(x_5)Q_5 - \Phi_i(x_1)Q_1]. \tag{1.8}$$

Consider the first term on the left hand side of equation (1.6), and denote it in matrix form as

$$AU = \sum_{r=1}^{4}\sum_{j=1}^{5} u_j \int\limits_{e_r} \frac{d\Phi_i}{dx}\frac{d\Phi_j}{dx}dx, \quad i = 1(1)5 \tag{1.9}$$

Evaluate the integral over an element e having nodes 1 and 2, we get

$$A^e = \begin{bmatrix} 1/L & -1/L \\ -1/L & 1/L \end{bmatrix} \tag{1.10}$$

where L is defined as distance between the nodes.

Consider the second term on the left hand side of equation (1.6), and denote it in matrix form as

$$BU = \sum_{r=1}^{4}\sum_{j=1}^{5} u_j \int\limits_{e_r} \Phi_i(x)\Phi_j(x)dx, \quad i = 1(1)5 \tag{1.11}$$

Again, evaluating the integral over element e, we get

$$B^e = \begin{bmatrix} L/3 & L/6 \\ L/6 & L/3 \end{bmatrix} \tag{1.12}$$

Adding (1.10) and (1.12), we get

$$P^e = \begin{bmatrix} 3 + L^2/3L & 6 - L^2/6L \\ -(6 - L^2)/6L & 3 + L^2/3L \end{bmatrix}$$

Substituting the values $L_1 = 0.2, L_2 = 0.3, L_3 = 0.3, L_4 = 0.2$, we get

$$P_1 = \begin{bmatrix} 15.2/3 & -14.9/3 \\ -14.5/3 & 15.2/3 \end{bmatrix}$$

$$P_2 = \begin{bmatrix} 15.2/3 & -14.9/3 \\ -14.5/3 & 15.2/3 \end{bmatrix}$$

Since $P_3 = P_2$ and $P_4 = P_1$. Since $L_3 = L_2$ and $L_4 = L_1$. Values of P_1, P_2, P_3, P_4 are inserted in appropriate rows and columns.

The *ith* term of the column vector R of equation (1.7) is given by

$$R_i = \int_0^1 x\phi_i(x)dx, \quad i = 1(1)5.$$

$$R_i^e = \sum_{r=1}^{4} \int\limits_{e_r} x\Phi_i(x)dx, \quad i = 1(1)5.$$

Evaluating the above integral over the element e having nodes 1 and 2.

$$R_1^e = \frac{1}{2}x_1 L + \frac{L^2}{6}$$
$$R_2^e = \frac{1}{2}x_1 L - \frac{L^2}{6}$$

Similarly, we can get the expression for R over other elements.

$$R = \begin{bmatrix} \frac{1}{2}x_1 L_1 + \frac{L_1^2}{6} \\ \frac{1}{2}x_2 L_1 + \frac{L_1^2}{6} + \frac{1}{2}x_2 L_2 - \frac{L_2^2}{6} \\ \frac{1}{2}x_3 L_2 + \frac{L_2^2}{6} + \frac{1}{2}x_3 L_3 - \frac{L_3^2}{6} \\ \frac{1}{2}x_4 L_3 + \frac{L_3^2}{6} + \frac{1}{2}x_4 L_4 - \frac{L_4^2}{6} \\ \frac{1}{2}x_5 L_4 + \frac{L_4^2}{6} \end{bmatrix}$$

$$R = \begin{bmatrix} 0.00667 \\ 0.05833 \\ 0.15 \\ 0.19167 \\ 0.09333 \end{bmatrix}$$

Given that, $Q_5 = -1$,

Using nodal values for $x_1 = 0, x_2 = 0.2, x_3 = 0.5, x_4 = 0.8, x_5 = 1.0$, in $T_i = [-\Phi_i(x_5)Q_5 + \Phi_i(x_1)Q_1]$, we get

$$T = \begin{bmatrix} Q_1 \\ 0 \\ 0 \\ 0 \\ -1 \end{bmatrix}$$

Using the values of $P_1, P_2, P_3, P_4, P_5, R$ and T, the system (1.6) becomes

$$5.0667u_1 - 4.9667u_2 = 0.00667 - Q_1$$
$$-4.9667u_1 + 8.5u_2 - 3.2833u_3 = 0.05833$$
$$-3.2833u_2 + 6.8667u_3 - 3.28337u_4 = 0.15$$
$$-3.2833u_3 + 8.5u_4 - 4.9669u_5 = 0.191667$$
$$-4.9667u_4 + 5.0667u_5 = 1.0933.$$

Since Q_1 is not known, therefore we neglect first equation and consider the above remaining equations. Since $u_1 = 1$ is given, solving these linear equations, we get

$$u_2 = 1.0667 \quad u_3 = 1.2307$$

$$u_4 = 1.4610 \quad u_5 = 1.6480$$

Now, computing Q_1 from first equation, we get

$$Q_1 = 0.2355.$$

1.9 Element free methods

Traditionally, complex partial differential equation are largely solved using numerical methods, such as finite element method (FEM) and finite difference method (FDM) [13]. In these methods, the special domain where the partial differential governing equations are defined is often discretized into meshes.

A mesh is defined as any of the open spaces or interstices between the stands of a net that is formed by connecting nodes in a predefined manner.In FDM, the meshes used are also often called grids; in the finite volume method (FVM), the meshes are called volumes or cells; and in FEM, the meshes are called elements. The terminologies of grids, volumes, cells, and element carry certain physical meanings as they are defined for different physical problems. However, all these grids, volumes, cells, and elements can be termed meshes according to the above definition of mesh. The key here is that a mesh must be predefined to provide certain relationship between the nodes, which is the base of the formulation of these conventional numerical methods.

By using a properly predefined mesh and by applying a proper principle, complex differential or partial differential governing equations can be approximated by a set of algebraic equations for the mesh. The system of algebraic equations for the whole problem domain can be formed by assembling set of algebraic equations for all the meshes.

The mesh free method [15], abbreviated element free, is used to establish a system of algebraic equations for the whole problem domain without the use of predefined mesh. Element free methods use a set of nodes scattered within the problem domain as well as sets of nodes scattered on the boundaries of the domain to represent the problem domain and its boundaries.

These sets of scattered nodes do not form a mesh, which means that no information on the relationship between the nodes is required, at least for field variable interpolation.
There are number of element free methods [15], such as the element free Galerkin (EFG) method, the meshless local Petrov-Galerkin (MLPG) method, the point interpolation method (PIM), etc. They all share the same feature that predefined meshes are not used. In contrast to FEM, the term element free method is preferred.

The minimum requirement for an element free method:

- That a predefined mesh is not necessary, at least in field variable interpolation.

The ideal requirement for an element free method:

- That no mesh is necessary at all throughout the process of solving the problem of given arbitrary geometry governed by partial differential system equations subject to all kinds of boundary conditions.

1.9.1 Need for element free methods

The need for the element free Galerkin methods is because of the following main reasons [15]:

1. Creation of a mesh for the problem domain is a prerequisite in using FEM packages. Usually the analyst spends the majority of his or her time in creating the mesh, and it becomes a major component of the cost of a simulation project because the cost of CPU time is drastically decreasing. The concern is more the manpower time, and less the computer time. Therefore, ideally the meshing process would be fully performed by the computer without human intervention.

2. When handling large deformation, considerable accuracy is lost because of the element distortions.

3. It is very difficult to simulate both crack growth with arbitrary and complex paths and phase transformation due to discontinuities that do not coincide with the original nodal lines.

4. It is very difficult to simulate the breakage of material into large number of fragments as FEM is essentially based on continuum mechanics, in which the elements formulated cannot be broken. The elements can stay as a whole piece. This usually leads to a misrepresentation of breakage path. Serious error can occur because the nature of the problem is non-linear, and therefore the results are highly path dependent.

5. In stress calculations, the stresses obtained using FEM packages are discontinuous and less accurate.

1.9.2 The idea of element free methods

All the difficulties associated with FEM reveals the root of the problem: the need to use elements, which are the building block of FEM. A mesh with predefined ”connectivity” is required to form the elements. The concept of element free or mesh free methods [15] has been proposed, in which the domain of the problem is represented by a set of arbitrary distributed nodes. The mesh free method has great potential for solving the difficult problems. Adaptive schemes can be easily developed, as there is no mesh, and hence no connectivity concept involved. Thus there is no need to provide a priori any information about the relationship of the nodes. This provides flexibility in adding or deleting points/nodes whenever and wherever needed. In crack growth problems, nodes can be easily added around the crack tip to capture the stress concentration with desired accuracy. This nodal refinement can be moved with a propagation crack through a background arrangement of nodes associated with the global geometry.

Chapter 2

Element free Galerkin solution of radiative hydromagnetic micropolar flow saturated Darcy medium with heat transfer over a stretching sheet with Joule heating (Review of research paper)

2.1 Introduction

Multiphysical porous media thermofluid dynamics continues to attract the attention of the applied mathematics and engineering science research communities because of increasing applications in many branches of chemical and mechanical engineering. Both Newtonian and non-Newtonian heat and momentum transfer in conducting or nonconducting saturated porous system constitute many of the fundamental flows encountered in for example, silicon carbide porous media composite synthesis [27], evaporating and drying capillary porous material systems [16], etc. In high-temperature chemical engineering operations, it also becomes necessary to simulate thermal radiation heat transfer effects. For example, Wu et al. [22] studied radiative-conductive heat transfer with in porous polymer materials. Many theoretical models have been developed for radiative convention flows and radiative conductive transport. In stretching sheet processes, the radiative heat transfer properties of the cooling medium may also be manipulated to judiciously influence the rate of cooling. Many other effects also be used such as porosity of the medium. Different thermophysical effects may also be employed to obtain best results. This is restricted to Newtonian viscous models. Non-Newtonian that is, rheological flow are however significant in many porous and nonporous media. Eringen [9] introduced the theory of microfluids because rheological fluids are not capable of simulating the microstructure characteristics of certain chemical suspension. Eringen [10] later developed the theory of micropolar fluids for the case where only micro rotational effects and micro rotational inertia exist. In the present study, we analyze numerically the steady, hydro-magnetic flow and heat transfer in a conducting micropolar fluid from a semi-infinite stretching sheet through porous medium incorporating viscous heating and radiative heat transfer effects. A drag force formulation is employed to simulate porous media effects. The mathematical modal developed is highly nonlinear and the element free Galerkin method (EFGM) is employed to solve the model problem .

Micropolar fluids are fluids with microstructure belonging to a class of complex fluids with non-symmetrical stress tensor referred to as micromorphic fluids. The general form of the equations for micropolar fluid, in Gibbsian vector notation can be stated following Eringen [10] as follows:

Conservation of mass:

$$\frac{\partial \rho}{\partial t} + \Delta.(\rho\chi) = 0 \tag{2.1}$$

Conservation of translational momentum:

$$\begin{aligned}(\lambda + 2\mu + \chi)\nabla\nabla.V - (\mu + \chi)\nabla \times \nabla \times V + \chi\nabla \times N - \nabla P + \rho f \\ = \frac{\partial V}{\partial t} - V \times (\nabla \times V) + \frac{1}{2}\nabla V^2\end{aligned} \tag{2.2}$$

Consevation of angular momentum:

$$(\alpha + \beta + \gamma)\nabla\nabla.N - \gamma\nabla \times \nabla \times N + \chi\nabla \times V - 2\chi N + \rho I = \rho j N \tag{2.3}$$

where λ, μ, α, β, χ and γ are viscosity coefficients of micropolar fluid, P is pressure, V is translational velocity vector, N is microrotation vector and ρ is the mass density of micropolar fluid. In micropolar model theory we are only concerned with velocity vector field that is familiar from Navier-Stokes theory and the axial vector field that represents the spin of the micropolar fluid particles, both fields are independent, these being assumed rigid. Here we implement the following simplified version of the previous model, where, microrotation about only one axis is modeled:

$$(1+K)f''' + ff'' - (f')^2 + Kg' - \frac{1+K}{\varepsilon}f' - Mf' = 0 \tag{2.4}$$

$$\left(1+\frac{K}{2}\right)g'' + fg' - f'g - K(2g+f'') = 0 \tag{2.5}$$

$$\frac{1}{Pr}\left(\frac{1}{R}+1\right)\Theta'' + f\Theta' + Ec(1+K)\left((f'')^2 + \frac{1}{\varepsilon}(f')^2\right) + EcM(f')^2 = 0 \tag{2.6}$$

and the corresponding boundary conditions are given by:

$$\begin{aligned} &f = 0, f' = 1, g = -sf'', \Theta = 1 \text{ at } \eta = 0 \\ &f' \longrightarrow 0, g \longrightarrow 0, \Theta \longrightarrow 0 \;\; at \;\; \eta \longrightarrow \infty \end{aligned} \tag{2.7}$$

where the primes denote differentiation with respect to η (non-dimensional y-coordinate) and $K = \dfrac{k}{\rho\nu}$ is the Eringen micropolar parameter, $M = \dfrac{\sigma B_0^2}{\rho D}$ is magnetic number (where D is the dimensional constant), $Pr = \dfrac{\rho\nu c_p}{k_f}$ is number , $Ec = \dfrac{u_w^2}{c_p}(T_w - T_\infty)$ is the Eckert number, ε is the porosity, T_w is wall temperature, T_∞ is free-stream temperature, s is the surface condition parameter and varies from 0 to 1, and $R = \dfrac{3k^* k_f}{16\sigma^* T_\infty^3}$ denote the Boltzmann Rosseland conduction-radiation number. This last parameter embodies the relative contribution of heat transfer by thermal conduction to thermal radiation in flow regime. Large $R(>1)$ values, therefore, correspond to thermal conduction dominance and small values (< 1) to thermal radiation dominance. For $R = 1$ both conduction and radiative heat transfer modes will contribute equally to the regime. Clearly, the first term in heat equation (2.6) is an augmented diffusion term. The coefficient of Θ'' shows that as $R \longrightarrow \infty$, then $\left(\dfrac{1}{R}+1\right) \longrightarrow 1$, that is thermal radiation contribution vanishes and equation (2.6) reduces to the non-radiative thermal energy equation. Hence, for very small R, thermal radiation will be significant and conduction will be negligible and vice versa for large R. We expect, with small R therefore, that greater radiative energy will be imparted to the flow that will heat the fluid and elevate temperatures.

2.2 Numerical study using element free Galerkin method

The system of ordinary differential equations defined by (2.4) to (2.6) is highly nonlinear. Analytical solution is intractable for the present system. We therefore, seek a numerical solution. The finite element method (FEM) has been extensively applied in numerical computations dealing in micropolar flow [1]-[21]. Although FEM is very versatile numerical method, there are intrinsic challenges involving discretization, meshing and remeshing of complex geometries of the problems that can incur excessive computational costs. To overcome these problems, a number of meshless methods have been developed in last two decades. Among all the meshless methods, the element free Galerkin method EFGM has been successfully utilized to solve various problems in diverse branches of engineering including fracture mechanics [3], static and dynamics fracture [4], heat transfer [20], electro-magnetics fields [6], wave propagation [32], and fluid flow [25]-[24] etc. EFGM have the following differences over FEM:

1. There is no element mesh involved in the discretization process.
2. Node creation and elemination is relatively easier than FEM.
3. Creation of shape function is based on nodes.
4. Shape functions may not satisfy Kronecker delta condition.
5. Selection of basis function is more flexible than FEM.
6. Complex geometries and moving domain problems can be easily handled.
7. Good accuracy and high convergence rate can be achieved.

The advantages of element free Galerkin methods (EFGM) over finite element methods motivated many researchers to extend the application of element free Galerkin method to coupled nonlinear flow and heat transfer problems. Therefore, in the present study, EFGM has been used for numerical simulation. The EFGM requires moving least square (MLS) interpolation functions to approximate an unknown function, which contains three components: basis functions, weight functions associated with each node, and a set of coefficients that depend on position of the nodes. The weight function is non zero over a small neighborhood at a particular node, which is known as the support of the node. By using MLS approximation, the unknown velocity component $f(x)$ is approximated. Let $f(x)$ be the function of field variable defined in the domain $[0, \infty]$. The approximation of $f(x)$ at a point x is denoted by $f^h(x)$. MLS approximation first writes the field function in the form:

$$f(x) \cong f^h(x) = \sum_{j=1}^{m} p_j(x)a_j(x) = p^T(x)a(x) \tag{2.8}$$

where m is the number of terms in basis functions, $p_j(x)$ is the monomial basis function, $a_j(x)$ the nonconstant coefficients, and $p^T(x) = [1 \ \ x]$.

A function of weighted residual is constructed using approximated values of the field function and the nodal parameters f_I. The coefficients $a_j(x)$ are determined by minimizing the function $J(x)$ which is defined as:

$$J(x) = \sum_{I=1}^{n} w(x - x_I) \left(\sum_{j=1}^{m} p_j(x_I)a_j(x) - f_I \right)^2 \tag{2.9}$$

where $w(x - x_I)$ are weight functions that are nonzero over a small domain, known as the domain of influence, n number of nodes in domain of influence. The influence domain is defined as a domain that a node exerts an influence upon. It goes with a node, in contrast to the support domain, which goes with point of interest x that can be, but does not necessarily have to be, at the node. Fig1. shows the node configuration and the difference between approximate function $f^h(\eta_I)$ and the nodal parameter f_I associated with each node $I(I = 1, 2, 3, ...n)$.

The minimization of $J(x)$ with respect to $a(x)$ generates the following set of equations:

$$a(x) = C^{-1}(x)D(x)f \tag{2.10}$$

where C and D are defined as follows:

$$C = \sum_{I=1}^{n} w(x - x_I)p(x_I)p^T(x_I) \tag{2.11}$$

$$D(x) = [w(x - x_1)p(x_1), w(x - x_2)p(x_2), ..., w(x - x_n)p(x_n)] \tag{2.12}$$

$$f = [f_1, f_2, ..., f_n]^T. \tag{2.13}$$

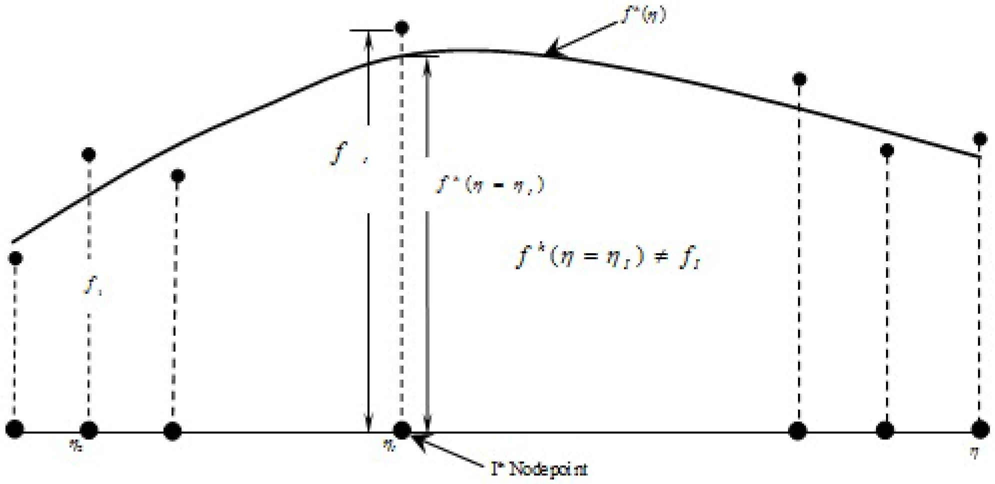

Figure 1: Node configuration and difference between f_I and $f^*(\eta_I)$

Substituting equation (2.10) in equation (2.8), the MLS approximation is obtained as follow:

$$f(x) \cong f^h(x) = \sum_{I=1}^{n} \Phi_I(x) f_I = \Phi(x) f \tag{2.14}$$

where the shape functions $\Phi_I(x)$ are defined by the following:

$$\Phi_I(x) = \sum_{j=1}^{n} p_j(x)(C^{-1}(x)D(x))_{jI} = p^T C^{-1} D_I. \tag{2.15}$$

Similarly, the other unknown functions, micro-rotation (g), and temperature (Θ) can be approximated.

2.2.1 Choice of weight functions

The weight function $w(x - x_I)$ over a small neighborhood of x_I is nonzero, which is called domain of influence of node I. The choice of weight function affects the resulting approximation in EFGM and other meshless methods. Singh et al. [19] has made a study on these weight functions and found that the cubic spline weight function ensures greater accuracy results as compared with other weight functions. Therefore, in the present work, a cubic spline weight function is adopted which is defined as follows:

$$w(x-x_I) \equiv w(\overline{d}) = \begin{cases} \frac{2}{3} - 4\overline{d}^2 + 4\overline{d}^3 & for \;\; \overline{d} \leq \frac{1}{2} \\ \frac{4}{3} - 4\overline{d} + 4\overline{d}^2 - \frac{4}{3}\overline{d}^3 & for \;\; \frac{1}{2} < \overline{d} < 1 \\ 0 & for \;\; \overline{d} > 1. \end{cases}$$

where $\overline{d} = \frac{||x-x_I||}{d_w} = \frac{d}{d_w}$ and d_w is directly related to smoothing length h. The smoothing length controls the size of the compact support domain, which is often termed as the influence domain or smoothing domain.

2.2.2 Essential boundary conditions

In element free Galerkin method, there is lack of Kronecker delta property, because of which the shape functions Φ_I poses some difficulty in imposition of the essential boundary conditions. To remove this problem, different numerical techniques have been proposed to enforce the essential boundary conditions in EFGM such as modified variational principle approach, Lagrange multiplier technique, Penalty approach, and so on.

To solve equations (2.4) to (2.6) by using element free Galerkin method, it is assumed that

$$f' = h \tag{2.16}$$

Substituting equation (2.16) into equations (2.4) to (2.6), we obtain

$$(1+K)h'' + fh' - (h)^2 + Kg' - \frac{1+K}{\varepsilon}h - Mh = 0 \tag{2.17}$$

$$\left(1+\frac{K}{2}\right)g'' + fg' - hg - K(2g+h') = 0 \tag{2.18}$$

$$\frac{1}{Pr}\left(\frac{1}{R}+1\right)\Theta'' + f\Theta' + Ec(1+K)\left((h')^2 + \frac{1}{\varepsilon}(h)^2\right) + EcM(h)^2 = 0 \tag{2.19}$$

and the corresponding boundary conditions reduces to the

$$\begin{gathered} f=0, h=1, g=-sh', \Theta=1 \quad at \quad \eta=0 \\ h \longrightarrow 0, g \longrightarrow 0, \Theta \longrightarrow 0 \quad at \quad \eta \longrightarrow \infty. \end{gathered} \tag{2.20}$$

The variational form associated with equations (2.16) to (2.19) over entire domain $(0, \eta_\infty)$ can be written as

$$\int_0^{\eta_\infty} w_1(f' - h)d\eta = 0 \tag{2.21}$$

$$\int_0^{\eta_\infty} w_2\left((1+K)h'' + fh' - (h)^2 + Kg' - \frac{1+K}{\varepsilon}h - Mh\right)d\eta = 0 \tag{2.22}$$

$$\int_0^{\eta_\infty} w_3\left(\left(1+\frac{K}{2}\right)g'' + fg' - hg - K(2g + h')\right)d\eta = 0 \tag{2.23}$$

$$\int_0^{\eta_\infty} w_4\left(\frac{1}{Pr}\left(\frac{1}{R}+1\right)\Theta'' + f\Theta' + Ec(1+K)\left((h')^2 + \frac{1}{\varepsilon}(h)^2\right) + EcM(h)^2\right)d\eta = 0, \tag{2.24}$$

where w_1, w_2, w_3 *and* w_4 are arbitrary test functions and may be viewed as variation in f, h, g and Θ respectively. We use weak formulation to simplify these equations.

From equation (2.22), we get

$$\begin{aligned}
&\int_0^{\eta_\infty} w_2\left((1+K)h'' + fh' - (h)^2 + Kg' - \frac{1+K}{\varepsilon}h - Mh\right)d\eta = 0\\
&\int_0^{\eta_\infty} w_2(1+K)h''d\eta + \int_0^{\eta_\infty} w_2\left(fh' - (h)^2 + Kg' - \frac{1+K}{\varepsilon}h - Mh\right)d\eta = 0\\
&[w_2(1+K)h']_0^{\eta_\infty} - \int_0^{\eta_\infty} w_2'(1+K)h'd\eta + \int_0^{\eta_\infty} w_2(fh' - h^2 + kg - \frac{1+K}{\varepsilon}h'\\
&\qquad -Mh)d\eta = 0.
\end{aligned} \tag{2.25}$$

From equation (2.23), we get

$$\begin{aligned}
&\int_0^{\eta_\infty} w_3\left(\left(1+\frac{K}{2}\right)g'' + fg' - hg - K(2g + h')\right)d\eta = 0\\
&\int_0^{\eta_\infty} w_3\left(1+\frac{K}{2}\right)g''d\eta + \int_0^{\eta_\infty} w_3(fg' - hg - K(2g + h'))d\eta = 0\\
&\left[w_3\left(1+\frac{K}{2}\right)g'\right]_0^{\eta_\infty} - \int_0^{\eta_\infty} w_3'\left(1+\frac{K}{2}\right)g'd\eta + \int_0^{\eta_\infty} w_3(fg' - hg\\
&\qquad -K(2g + h'))d\eta = 0.
\end{aligned} \tag{2.26}$$

From equation (2.24), we get

$$\int_0^{\eta_\infty} w_4 \left(\frac{1}{Pr} \left(\frac{1}{R} + 1 \right) \Theta'' + f\Theta' + Ec(1+K) \left((h')^2 + \frac{1}{\varepsilon}(h)^2 \right) + EcM(h)^2 \right) d\eta = 0$$

$$\int_0^{\eta_\infty} w_4 \frac{1}{Pr} \left(\frac{1}{R} + 1 \right) \Theta'' d\eta + \int_0^{\eta_\infty} w_4 (f\Theta' + Ec(1+K) \left((h')^2 + \frac{1}{\varepsilon}(h)^2 \right) + EcM(h)^2) d\eta = 0$$

$$\left[w_4 \frac{1}{Pr} \left(\frac{1}{R} + 1 \right) \Theta' \right]_0^{\eta_\infty} - \int_0^{\eta_\infty} w_4' \frac{1}{Pr} \left(\frac{1}{R} + 1 \right) \Theta' d\eta + \int_0^{\eta_\infty} w_4 (f\Theta' + Ec(1+K) \left((h')^2 + \frac{1}{\varepsilon}(h)^2 \right) + EcM(h)^2) d\eta = 0. \tag{2.27}$$

Now, using essential boundary conditions on w_1, w_2, w_3, w_4 as homogeneous conditions, equations (2.21), (2.25), (2.26), (2.27) become

$$\int_0^{\eta_\infty} w_1 (f' - h) d\eta = 0 \tag{2.28}$$

$$\int_0^{\eta_\infty} \left(-w_2'(1+K)h' + w_2 f h' - w_2 (h)^2 + w_2 K g' - w_2 \frac{1+K}{\varepsilon} h - w_2 M h \right) d\eta = 0 \tag{2.29}$$

$$\int_0^{\eta_\infty} \left(-w_3' \left(1 + \frac{K}{2} \right) g' + w_3 f g' - w_3 h g - w_3 K (2g + h') \right) d\eta = 0 \tag{2.30}$$

$$\int_0^{\eta_\infty} \left(-w_4' \frac{1}{Pr} \left(\frac{1}{R} + 1 \right) \Theta' + w_4 f \Theta' + w_4 Ec(1+K) \left((h')^2 + \frac{1}{\varepsilon}(h)^2 \right) + w_4 EcM(h)^2 \right) d\eta = 0. \tag{2.31}$$

Next, the equations (2.28) to (2.31) are linearized by incorporating function $\overline{f}, \ \ \overline{g}, \ \ and \ \ \overline{h}$ where

$$\overline{f} = \sum_{I=1}^{n} \overline{f}_I \Phi_I, \quad \overline{h} = \sum_{I=1}^{n} \overline{h_I} \Phi_I, \quad \overline{g} = \sum_{I=1}^{n} \overline{g_I} \Phi_I. \tag{2.32}$$

Now, in order to enforce essential boundary conditions, the penalty method in accordance with Zhu and Alturi [30] is applied as follows:

From equation (2.28), we get

$$\int_0^{\eta_\infty} w_1(f'-h)d\eta + \alpha w_1(f-f_0)|_{\eta=0} = 0$$

$$\int_0^{\eta_\infty} \Phi_I \left(\sum_{J=1}^{n} \Phi'_J f_J - \sum_{J=1}^{n} \Phi_J h_J\right) d\eta + \alpha\Phi_I \left(\sum_{J=1}^{n} \Phi_J f_J - f_0\right)|_{\eta=0} = 0$$

$$\sum_{J=1}^{n}\int_0^{\eta_\infty} \Phi_I\Phi'_J f_J d\eta - \sum_{J=1}^{n}\int_0^{\eta_\infty} \Phi_I\Phi_J h_J d\eta + \alpha\sum_{J=1}^{n} \Phi_I\Phi_J f_J|_{\eta=0} - \alpha f_0\Phi_I|_{\eta=0} = 0$$

$$\int_0^{\eta_\infty} \left(\Phi_I^T\Phi'_J d\eta + \alpha\Phi_I^T\Phi_J|_{\eta=0}\right) f_J - \int_0^{\eta_\infty} \Phi_I^T\Phi_J h_J d\eta = \alpha f_0\Phi_I|_{\eta=0}. \tag{2.33}$$

From equation (2.29), we get

$$\int_0^{\eta_\infty} \left(-w_2'(1+K)h' + w_2\overline{f}h' - w_2\overline{h}h + w_2Kg' - w_2\frac{1+K}{\varepsilon}h - w_2Mh\right) d\eta$$
$$+\alpha w_2(h-h_0)|_{\eta=0} + \alpha w_2(h-h_\infty)|_{\eta=\infty} = 0$$

$$\int_0^{\eta_\infty} \left(-\Phi_I'(1+K)\sum_{J=1}^{n}\Phi'_J h_J + \Phi_I\overline{f}\sum_{J=1}^{n}\Phi'_J h_J - \Phi_I\overline{h}\sum_{J=1}^{n}\Phi_J h_J + \Phi_I K\sum_{J=1}^{n}\Phi'_J g_J\right.$$
$$\left.-\Phi_I\frac{1+K}{\varepsilon}\sum_{J=1}^{n}\Phi_J h_J - \Phi_I M\sum_{J=1}^{n}\Phi_J h_J\right) d\eta + \alpha\Phi_I\sum_{J=1}^{n}\Phi_J h_J|_{\eta=0} - \alpha\Phi_I h_0|_{\eta=0}$$
$$+\alpha\Phi_I\sum_{J=1}^{n}\Phi_J h_J|_{\eta=\infty} - \alpha\Phi_I h_\infty|_{\eta=\infty} = 0$$

$$-\int_0^{\eta_\infty} \left(\Phi_I'^T(1+K)\sum_{J=1}^{n}\Phi'_J + \Phi_I^T\overline{h(\eta)}\Phi_J - \Phi_I^T\overline{f(\eta)}\Phi'_J + \Phi_I^T\frac{1+K}{\varepsilon}\Phi_J + \Phi_I^T M\Phi_J\right) h_J d\eta$$
$$+(\alpha\Phi_I^T\Phi_J|_{\eta=0} + \alpha\Phi_I^T\Phi_J|_{\eta=\infty})h_J + \int_0^{\eta_\infty} \Phi_I^T K\Phi'_J g_J d\eta = h_0\alpha\Phi_I|_{\eta=0} + h_\infty\alpha\Phi_I|_{\eta=\infty} \tag{2.34}$$

From equation (2.30), we get

$$\int_0^{\eta_\infty} \left(-w_3'\left(1+\frac{K}{2}\right)g' + w_3\overline{f}g' - w_3h\overline{g} - w_3K(2g+h')\right) d\eta$$
$$+\alpha w_3(g-g_0)|_{\eta=0} + \alpha w_3(g-g_\infty)|_{\eta=\infty} = 0$$

$$\int_0^{\eta_\infty} \left(-\Phi_I'\left(1+\frac{K}{2}\right)\sum_{J=1}^{n}\Phi'_J g_J + \Phi_I\overline{f(\eta)}\sum_{J=1}^{n}\Phi'_J g_J - \Phi_I\overline{g(\eta)}\sum_{J=1}^{n}\Phi_J h_J\right.$$
$$\left.-\Phi_I K\left(2\sum_{J=1}^{n}\Phi_J g_J + \sum_{J=1}^{n}\Phi'_J h_J\right)\right) d\eta + \alpha\Phi_I\left(\sum_{J=1}^{n}\Phi_J g_J - g_0\right)|_{\eta=0}$$
$$+\alpha\Phi_I\left(\sum_{J=1}^{n}\Phi_J g_J - g_\infty\right)|_{\eta=\infty} = 0$$

$$-\int_0^{\eta_\infty}\left(\Phi_I'^T\left(1+\frac{K}{2}\right)\Phi_J'-\Phi_I^T\overline{f(\eta)}\Phi_J'+2K\Phi_I^T\Phi_J\right)g_Jd\eta+(\alpha\Phi_I^T\Phi_J|_{\eta=0})g_J$$

$$+(\alpha\Phi_I^T\Phi_J|_{\eta=\infty})g_J-\int_0^{\eta_\infty}(\Phi_I^T\Phi_J\overline{g(\eta)}+K\Phi_I^T\Phi_J')h_Jd\eta=\alpha\Phi_Ig_0|_{\eta=0}+\alpha\Phi_Ig_\infty|_{\eta=\infty}\quad(2.35)$$

From equation (2.31), we get

$$\int_0^{\eta_\infty}\left(-w_4'\frac{1}{Pr}\left(\frac{1}{R}+1\right)\Theta'+w_4\overline{f}\Theta'+w_4Ec(1+K)\left(\overline{h'}h'+\frac{1}{\varepsilon}\overline{h}h\right)\right.$$

$$\left.+w_4EcM\overline{h}h\right)d\eta+\alpha w_4(\Theta-\Theta_0)|_{\eta=0}+\alpha w_4(\Theta-\Theta_\infty)|_{\eta=\infty}=0$$

$$\int_0^{\eta_\infty}\left(-\Phi_I'\frac{1}{Pr}\left(\frac{1}{R}+1\right)\sum_{J=1}^{n}\Phi_J'\Theta_J+\Phi_I\overline{f(\eta)}\sum_{J=1}^{n}\Phi_J'\Theta_J\right.$$

$$+\Phi_IEc(1+K)\left(\overline{h'(\eta)}\sum_{J=1}^{n}\Phi_J'h_J+\frac{1}{\varepsilon}\overline{h(\eta)}\sum_{J=1}^{n}\Phi_Jh_J\right)$$

$$\left.+\Phi_IEcM\overline{h(\eta)}\sum_{J=1}^{n}\Phi_Jh_J\right)d\eta+\alpha\Phi_I(\sum_{J=1}^{n}\Phi_J\Theta_J-\Theta_0)|_{\eta=0}$$

$$+\alpha\Phi_I\left(\sum_{J=1}^{n}\Phi_J\Theta_J-\Theta_\infty\right)|_{\eta=\infty}=0$$

$$-\int_0^{\eta_\infty}\left(\Phi_I'^T\frac{1}{Pr}\left(\frac{1}{R}+1\right)\Phi_J'-\Phi_I^T\overline{f(\eta)}\Phi_J'\right)\Theta_Jd\eta+(\alpha\Phi_I^T\Phi_J|_{\eta=0}+\alpha\Phi_I^T\Phi_J|_{\eta=\infty})\Theta_J$$

$$+\int_0^{\eta_\infty}\left(\Phi_I^TEc(1+K)(\overline{h'(\eta)}\Phi_J'+\frac{1}{\varepsilon}\overline{h(\eta)}\Phi_J)+\Phi_I^TEcM\overline{h(\eta)}\Phi_J\right)h_Jd\eta$$

$$=\alpha\Phi_I\Theta_0)|_{\eta=0}+\alpha\Phi_I\Theta_\infty)|_{\eta=\infty}\quad(2.36)$$

where

$$f_0=0,\quad h_0=1,\quad g_0=-sh_0',\quad\Theta_0=1$$
$$h_\infty=0,\quad g_\infty=0,\quad\Theta_\infty=0\quad(2.37)$$
$$and\ \ w_1=w_2=w_3=w_4=\Phi_I\quad(I=1,2,...,n)$$

In the matrix form, equation (2.33)-(2.36) can be written as follows:

$$[K]\{\overline{h}\}=\{F\}\quad(2.38)$$

and the entries of the matrix K are given by

$$[K]=\begin{bmatrix}K_{11}&K_{12}&K_{13}&K_{14}\\K_{21}&K_{22}&K_{23}&K_{24}\\K_{31}&K_{32}&K_{33}&K_{34}\\K_{41}&K_{42}&K_{43}&K_{44}\end{bmatrix},\quad\{\overline{h}\}=\begin{bmatrix}\{f\}\\\{h\}\\\{g\}\\\{\Theta\}\end{bmatrix},\quad\{F\}=\begin{bmatrix}\{F_1\}\\\{F_2\}\\\{F_3\}\\\{F_4\}\end{bmatrix}$$

where

$$
\begin{aligned}
(K_{11})_{IJ} &= \int_0^{\eta_\infty} (\Phi_I^T \Phi'_J) d\eta + \alpha \Phi_I^T \Phi_J|_{\eta=0}, \\
(K_{12})_{IJ} &= -\int_0^{\eta_\infty} \Phi_I^T \Phi_J d\eta, \\
(K_{13})_{IJ} &= 0, \\
(K_{14})_{IJ} &= 0, \\
(K_{21})_{IJ} &= 0, \\
(K_{22})_{IJ} &= -\int_0^{\eta_\infty} \Big(\Phi_I'^T (1+K) \Phi'_J + \Phi_I^T \overline{h(\eta)} \Phi_J - \Phi_I^T \overline{f(\eta)} \Phi'_J \\
&\quad + \Phi_I^T \frac{1+K}{\varepsilon} \Phi_J + \Phi_I^T M \Phi_J \Big) d\eta + (\alpha \Phi_I^T \Phi_J|_{\eta=0} + \alpha \Phi_I^T \Phi_J|_{\eta=\infty}), \\
(K_{23})_{IJ} &= \int_0^{\eta_\infty} \Phi_I^T K \Phi'_J d\eta, \\
(K_{24})_{IJ} &= 0, \\
(K_{31})_{IJ} &= 0, \\
(K_{32})_{IJ} &= -\int_0^{\eta_\infty} (\Phi_I^T \Phi_J \overline{g(\eta)} + K \Phi_I^T \Phi'_J) d\eta, \\
(K_{33})_{IJ} &= -\int_0^{\eta_\infty} \left(\Phi_I'^T \left(1 + \frac{K}{2}\right) \Phi'_J - \Phi_I^T \overline{f(\eta)} \Phi'_J + 2K \Phi_I^T \Phi_J \right) d\eta \\
&\quad + (\alpha \Phi_I^T \Phi_J|_{\eta=0} + \alpha \Phi_I^T \Phi_J|_{\eta=\infty}), \\
(K_{34})_{IJ} &= 0, \\
(K_{41})_{IJ} &= 0, \\
(K_{42})_{IJ} &= \int_0^{\eta_\infty} \left(\Phi_I^T Ec(1+K)(\overline{h'(\eta)} \Phi'_J + \frac{1}{\varepsilon} \overline{h(\eta)} \Phi_J) + \Phi_I^T EcM \overline{h(\eta)} \Phi_J \right) d\eta, \\
(K_{43})_{IJ} &= 0, \\
(K_{44})_{IJ} &= -\int_0^{\eta_\infty} \left(\Phi_I'^T \frac{1}{Pr} \left(\frac{1}{R} + 1 \right) \Phi'_J - \Phi_I^T \overline{f(\eta)} \Phi'_J \right) d\eta \\
&\quad + (\alpha \Phi_I^T \Phi_J|_{\eta=0} + \alpha \Phi_I^T \Phi_J|_{\eta=\infty}), \\
(F_1)_I &= f_0 \alpha \Phi_I|_{\eta=0}, \\
(F_2)_I &= h_0 \alpha \Phi_I|_{\eta=0} + h_\infty \alpha \Phi_I|_{\eta=\infty}, \\
(F_3)_I &= g_0 \alpha \Phi_I|_{\eta=0} + g_\infty \alpha \Phi_I|_{\eta=\infty}, \\
(F_4)_I &= \Theta_0 \alpha \Phi_I|_{\eta=0} + \Theta_\infty \alpha \Phi_I|_{\eta=\infty}.
\end{aligned}
$$

Table 2.1: Values of $-\Theta'(0)$ for regular fluid for several values of Prandtl number with $M = 0$, $Ec = 0$, $R \to \infty$ and $\varepsilon \to \infty$.

				Present results	
Pr	$Ref.$[12]	$Ref.$[28]	$Ref.$[14]	$Numerical$	$Analytic$
0.72	0.4631	-	-	0.465041726	0.463144561
1	0.5820	0.5820	0.5820	0.582250705	0.581976707
3	1.1652	1.1652	1.1652	1.165168542	1.165245952
10	2.3080	-	2.3080	2.307516701	2.308003944

2.3 Results and discussion

The system of ordinary differential equations (2.4)-(2.6), together with their corresponding boundary conditions (2.7), is solved using EFGM and the results are provided graphically. Two-point Gaussian quadrature formula have been used to evaluate the integral values. Owing to the nonlinearity of the systems of equations an iterative scheme is required to solve the nonlinear algebraic matrix system. The system is linearized by incorporating known functions $\overline{f}$, $\overline{g}$, and $\overline{\Theta}$, which is solved efficiently employing the Gauss-Seidel technique while sustaining an accuracy of 0.0001. To verify the accuracy of the applied numerical scheme, comparisons of the present results corresponding to the values of heat transfer coefficient for regular fluid with $M = 0$, $Ec = 0$, $R \to \infty$ and $\varepsilon \to \infty$ are made with the available results of Grubka and Bobba [12], Mukhopadhyay and Gorla [28] and Ishak et al. [14] as well as the series solution given by equation a presented Table 1. The results are founded in an excellent agreement, and thus give confidence that the numerical results in our case are accurate.

We have presented selected results in Figs 2-5, these results cover the following range of thermophysical data: $1 \leq \varepsilon \leq 10$, $0.0 \leq R \leq 5.0$, $0.75 \leq Pr \leq 7.0$, $0.02 \leq Ec \leq 3.0$ and Eringen vortex viscosity parameter, K is taken to be constant at 0.2.

Figure 2 shows that the linear flow velocity is enhanced with an increase in the dimensionless porous medium parameter ε. It shows that with greater space in the regime for the micropolar to percolate in, there will be a decreased resistance to the flow, that is, a reduction in the drag acting on the flow regime. Inspection of the dimensionless momentum equation

(2.4) shows that the Darcian-modified drag force term, $-\frac{(K+1)}{\varepsilon}f'$ is inversely proportional to porosity function for a fixed Eringen micropolar parameter ($K = 0.2$). Therefore, as ε increases, the drag force decreases, and the flow is accelerated. The maximum velocity therefore accompanies the maximum porosity function value, that is, $\varepsilon = 10.0$ in Figure 2. It is therefore apparent that to regulate the flow, a lower porosity will clearly decelerate the micropolar fluid owing to a concomitant increase in porous medium drag force, that is, Darcian impedance.
With an increase in porosity, we observe in Figure 3 that the microrotation g, is strongly boosted at the sheet surface, that is, at $\eta = 0$. Microrotation is also elevated throughout the boundary layer - however as we approach the free stream, the porosity effect is negligible because all profiles converge. This indicates that increasing permeability of the regime allows greater volume for the micro-elements to sustain rotary motions and accelerates spin of these micro-elements. The condition, $s = 0.5$, corresponds to week concentrations to micro-elements. Further from the sheet surface, s will not exert any tangible influence on microrotation, and therefore increasing porosity will also have very little influence in the region far from the wall.

Figure 4 shows that the temperature, θ decreases as ε increases. With greater porosity, and less solid particles comprise the porous medium, that is, fibers diminish. This results in a reduction in conduction heat transfer that serves to depress temperatures in the micropolar fluid. Clearly with lower porosities as encountered in certain ceramics and dense filters, greater temperatures can be sustained in the stretching sheet regime. High permeability and porosity media are therefore excellent for cooling the micropolar stretching sheet boundary layer flow.

Figure 5 shows the effect of Prandtl number on temperature profiles above the sheet. Very weak magnetic field ($M = 0.05$) is present for Figure 5 and weak viscous and also Joule dissipation ($Ec = 0.02$). A rise in Prandtl number markedly reduces the temperature of the conducting micropolar fluid above the sheet. Pr signifies the ration of momentum diffusivity to thermal diffusivity. Higher Pr values imply a thinner thermal boundary layer thickness and more uniform temperature distributions across the boundary layer. Hence, the thermal boundary layer will be much less in thickness than the hydrodynamics (translational velocity) boundary layer. $Pr = 1$ implies that the thermal and velocity boundary layers are approximately equal in extent. Lower Pr fluids will possess higher thermal conductivities (and thicker thermal boundary layer structures) so that heat can diffuse away from the stretching sheet surface faster than for higher Pr fluids (thinner boundary layers). Physically the lower values of Pr correspond to air ($Pr = 0.72$) water-based solutions ($Pr = 1$) for water and $Pr > 3$ may be representative of non-Newtonian oils and plastics. Our EFGM computations correlate well with the early study by Elbade etal. Hence, Prandtl number can be used to increase the rate of cooling in conducting micropolar flows. We note again that excellent correlation is achieved between FEM and EFGM solutions as shown by the case for $Pr = 0.72$ in Figure 5.

.

.

Chapter 3

Numerical simulation of unsteady MHD flow and heat transfer of second grade fluid with viscous dissipation and Joule heating using element free approach (Review of research paper)

3.1 Introduction

In many fluids such as blood, dyes, ketchup, shampoo, mud, clay etc. the relation between stress and strain can't be simply described by Newton's law of viscosity and are usually called non-Newtonian fluids. The flows of such type of fluids have immense practical applications in polymer devolatisation, fermentation, plastic form processing and many others. To study the behavior of non-Newtonian fluids, various models have been proposed by many authors taking account of variations of their rheological properties. One of the most popular models for non-Newtonian fluids is the model of second order fluids which is given by

$$T = -pI + \mu A_1 + \alpha_1 A_2 + \alpha_2 A_1^2, \tag{3.1}$$

where T is the Cauchy stress tensor, p is the pressure, α_1 and α_2 are material constants, and A_1, A_2 are defined as

$$A_1 = (gradV) + (gradV)^T$$
$$A_2 = \frac{dA_1}{dt} + A_1.(gradV) + (gradV)^T.A_1$$

The sign of the material constants α_1 and α_2 is the subject of much controversy which was discussed by Dunn and Rajagopal [8]. Generally, in the literature, the fluid which satisfies (3.1) with $\mu > 0, \alpha_1 > 0, \alpha_1 + \alpha_2 = 0$ is known as second grade fluid while fluid with restriction $\mu > 0, \alpha_1 < 0, \alpha_1 + \alpha_2 \neq 0$ is termed as second order fluid. When $\mu > 0, \alpha_1 = \alpha_2 = 0$, (3.1) reduces to well-known constitutive relation of an incompressible Newtonian fluid.
The problem of flow and heat transfer due to continuously moving stretching surface through an ambient fluid have received much attention in past. Such problems find their applications over a broad spectrum of science and engineering discipline, for example, aerodynamic extrusion of plastic sheets, the cooling of an infinite metallic plate in a cooling bath, the boundary layer along a liquid film in condensation process, and paper production, etc. In the present study an attempt has been made to provide the numerical simulation of moment and heat transfer of a second grade viscoelastic fluid over an oscillatory stretching sheet. Although flow is induced by oscillatory stretching sheet in the present analysis but there does also exists a free stream velocity oscillation in time about a constant mean oscillatory flow [31]-[2]. The non-linear mathematical model of the problem is solved by a element free numerical technique known as element free Galerkin method which is a very powerful technique and has been successfully employed to solve various problems in various different areas such as heat transfer [23], fracture mechanics [3] etc. Recently, Singh and Bhargava [29] have applied EFGM for the simulation of an unsteady micropolar squeeze film flow. Result obtained with EFGM are compared with some results reported by Chen [7] and Grubka and Bobba [12] in Table 1 and excellent agreement has been observed between them.

3.1.1 Mathematical Analysis

Consider the two dimensional unsteady MHD flow of an incompressible viscoelastic fluid (obeying second grade model) in the presence of viscous dissipation and joule heating past an oscillatory stretching surface coinciding with the plate $y = 0$ and the flow being confined to the space $y > 0$.

The flow is generated by stretching of an elastic boundary sheet which is stretched back and forth periodically with velocity $u_w = bx \sin \omega t$ parallel to x axis, where b is the stretching rate and ω is the oscillation frequency of the sheet. x and y axis are taken as the coordinates along the sheet and the normal to it respectively. Further u and v are the velocity components along the x and y directions respectively, the fluid moves in the x direction with the velocity (u-component) equal to the velocity of the solid surface, whereas at the increasing distance from the surface, the velocity of the fluid approaches to zero asymptotically.

A constant magnetic field of strength B_0 is applied perpendicular to the stretching surface and the effect of the induced magnetic field is neglected. All the fluid properties are assumed to be isotropic and constant. With the usual boundary layer approximation, the governing equations for the unsteady magneto-hydrodynamic momentum and heat transfer for a second grade viscoelastic fluid in the presence of viscous dissipation and joule heating take the following form:

$$\frac{\partial u}{\partial x} + \frac{\partial \nu}{\partial y} = 0 \tag{3.2}$$

$$\frac{\partial u}{\partial t} + u\frac{\partial u}{\partial x} + \nu\frac{\partial u}{\partial y} = \nu\frac{\partial^2 u}{\partial y^2} + k_0\left(\frac{\partial^3 u}{\partial t \partial y^2} + \frac{\partial}{\partial x}\left(u\frac{\partial^2 u}{\partial y^2}\right) + \nu\frac{\partial^3 u}{\partial y^3} + \frac{\partial u}{\partial y}\frac{\partial^2 \nu}{\partial y^2}\right) - \frac{\sigma B_0^2}{\rho}u \tag{3.3}$$

$$\rho c_p\left(\frac{\partial T}{\partial t} + u\frac{\partial T}{\partial x} + \nu\frac{\partial T}{\partial y}\right) = K\frac{\partial^2 T}{\partial y^2} + \mu\left(\frac{\partial u}{\partial y}\right)^2 + \sigma B_0^2 u^2, \tag{3.4}$$

where μ, ν are the dynamic and kinematic viscosity of the fluid, ρ is the fluid density, σ is the electrical conductivity of the fluid, k_0 is the viscoelastic parameter of the fluid, K is the thermal conductivity of the fluid and c_p is the specific heat at constant pressure.

The following appropriate boundary conditions are employed on the velocity field:

$$u = u_w = bx \sin \omega t, \quad \nu = 0 \quad at \quad y = 0, \quad t > 0 \tag{3.5}$$

$$u = 0, \quad \frac{\partial u}{\partial y} = 0 \quad as \quad y \to \infty. \tag{3.6}$$

An augmented boundary condition for the longitudinal velocity gradient has been used in the (3.6) following Fosdick and Rajagopal [11] . Physical implication of this boundary condition is

the absence of shear stress in the free stream. Since (3.3) is a third order differential equation in u where as without the augmented boundary condition, only two boundary conditions are prescribed on u. Hence, without the augmented boundary condition in (3.6), the above system is ill-posed. In (3.5), both ω and b have the dimension $(time)^{-1}$. We assume, $S = \frac{\omega}{b}$ which denotes the ratio of oscillation frequency of the sheet to its stretching rate.
The boundary condition for the temperature field are given as follows:

$$T = T_w = T_\infty + A\left(\frac{x}{l}\right)^2 \quad at \quad y = 0 \tag{3.7}$$

$$T \to T_\infty \quad as \quad y \to \infty, \tag{3.8}$$

where A is a constant and l is the characteristic length.

To examine the flow regime adjacent to the sheet, the following transformations are invoked,

$$\begin{aligned} &\eta = \sqrt{\frac{b}{\nu}}y, \quad \tau = t\omega, \\ &u = bxf_\eta(\eta,\tau), \quad \nu = -\sqrt{\nu b}f(\eta,\tau), \quad \theta(\eta,\tau) = \frac{T - T_\infty}{T_W - T_\infty}. \end{aligned} \tag{3.9}$$

Using transformations (3.9), the continuity equation is automatically satisfied and the governing equations (3.3) and (3.4) are reduced to following non-dimensional form:

$$Sf_{\eta\tau} + f_\eta^2 - ff_{\eta\eta} + M^2 f_\eta = f_{\eta\eta} + k_1(Sf_{\eta\eta\eta\tau} + 2f_\eta f_{\eta\eta\eta} - f_{\eta\eta}^2 - f_{\eta\eta\eta\eta}) \tag{3.10}$$

$$S\theta_\tau + 2f_\eta\theta - f\theta_\eta - \frac{1}{Pr}\theta_{\eta\eta} = Ecf_{\eta\eta}^2 + M^2 Ecf_\eta^2. \tag{3.11}$$

And the corresponding boundary conditions are transformed to

$$\begin{aligned} f_\eta(0,\tau) = \sin\tau, \quad f(0,\tau) = 0, \quad \theta(0,\tau) = 1, \\ f_\eta(\infty,\tau) = 0, \quad f_{\eta\eta}(\infty,\tau) = 0, \quad \theta(\infty,\tau) = 0, \end{aligned} \tag{3.12}$$

where $Pr = \frac{\mu c_p}{K}$ is the Prandtl number, $k_1 = \frac{k_0 b}{\nu}$ is the dimensionless viscoelastic parameter. Here $k_1 = 0$ corresponds to the case of a Newtonian fluid. $M^2 = \frac{\sigma B_0^2}{\rho b}$ is the Hartman number or the magnetic parameter and $Ec = \frac{b^2 l^2}{Ac_p}$ is the Eckert number.

For the solution of the system of simultaneous differential equations as given in (3.10) and(3.11), with the conditions (3.12), the equations are reformulated as:

$$\begin{aligned}
&f_\eta - h = 0,\\
&Sh_\tau + h^2 - fh_\eta + M^2h - h_\eta - k_1(Sh_{\eta\eta\tau} + 2hh_{\eta\eta} - h_\eta^2 - h_{\eta\eta\eta}) = 0,\\
&S\theta_\tau + 2h\theta - f\theta_\eta - \frac{1}{Pr}\theta_{\eta\eta} = Ech_\eta^2 + M^2Ech^2.
\end{aligned} \tag{3.13}$$

And the corresponding boundary conditions are:

$$\begin{aligned}
h(0,\tau) = \sin\tau, \quad f(0,\tau) = 0, \quad \theta(0,\tau) = 1,\\
h(\infty,\tau) = 0, \quad h_\eta(\infty,\tau) = 0, \quad \theta(\infty,\tau) = 0.
\end{aligned} \tag{3.14}$$

The system of simultaneous differential equations given in (3.13), along with boundary conditions (3.14), is numerically solved using Element Free Galerkin Method (EFGM).

3.1.2 Element free Galerkin method

The element free Galerkin method (EFGM) requires Moving least square (MLS) interpolation functions to approximate the unknown function. The MLS approximation requires only the set of nodes for its constructions and is made up of three components: a compact support weight function associated with each node, a polynomial basis function and a set of coefficients that depend upon node position. The weight function is non zero over a small neighborhood at a particular node, called support domain of the node. Using MLS approximation, the unknown field variable $u(x)$ is approximated over the domain Ω as

$$u(x) \cong u^h(x) = \sum_{j=1}^{m} p_j(x)a_j(x) = p^T(x)a(x), \tag{3.15}$$

where m is number of terms in basis, $p_j(x)$ the monomial basis function and $a_j(x)$ are the non-constant coefficient functions. In the present simulation, quadratic basis functions are used i.e. $p^T(x) = [1 \;\; x \;\; x^2]$. The coefficients $a_j(x)$ are determined by minimizing the function $J(x)$ given by:

$$J(x) = \sum_{I=1}^{n} w(x - x_I)\left(\sum_{j=1}^{m} p_j(x_I)a_j(x) - u_I\right)^2 \tag{3.16}$$

where $w(x - x_I)$ are weight functions that are nonzero over a small domain, denoted the domain of influence, n number of nodes in support domain. The minimization of $J(x)$ with respect to $a(x)$ generates the following set of equations:

$$a(x) = A^{-1}(x)B(x)U_s, \tag{3.17}$$

where A and B are given as

$$\begin{aligned} A(x) &= \sum_{I=1}^{n} w(x - x_I)p(x_I)p^T(x_I), \\ B(x) &= [w(x - x_1)p(x_1), w(x - x_2)p(x_2), ..., w(x - x_n)p(x_n)], \\ U_s &= [u_1, u_2, ..., u_n]^T. \end{aligned}$$

Substituting (3.17) in (3.15), the MLS approximation is obtained as:

$$u(x) \cong u^h(x) = \sum_{I=1}^{n} \Phi_I(x)u_I = \Phi(x)u, \tag{3.18}$$

where the shape function $\Phi_I(x)$ are defined by the following:

$$\Phi_I(x) = \sum_{j=1}^{n} p_j(x)(A^{-1}(x)B(x))_{jI} = p^T A^{-1} B_I; \quad I = 1, 2, ..., n. \tag{3.19}$$

3.1.3 Weight function description

The weight function $w(x - x_I)$ over a small neighborhood of x_I is nonzero, which is called domain of influence of node I. The choice of weight function affects the resulting approximation in EFGM and other meshless methods. Singh et al.[19] has made a study on these weight functions and found that the cubic spline weight functions ensure greater accuracy results as compared with other weight functions. Therefore, in the present work, cubic spline weight functions are adopted which are defined as follows:

$$w(x - x_I) \equiv w(\overline{d}) = \begin{cases} \frac{2}{3} - 4\overline{d}^2 + 4\overline{d}^3 & for \;\; \overline{d} \leq \frac{1}{2} \\ \frac{4}{3} - 4\overline{d} + 4\overline{d}^2 - \frac{4}{3}\overline{d}^3 & for \;\; \frac{1}{2} < \overline{d} < 1 \\ 0 & for \;\; \overline{d} > 1 \end{cases}$$

where $\overline{d} = \dfrac{||x - x_I||}{d_w} = \dfrac{d}{d_w}$ and d_w is directly related to smoothing length h. The smoothing length controls the size of the compact support domain, which is often termed as the influence domain or smoothing domain.

3.1.4 Variational Formulation

The weighted integral form of the equation (3.13) over the entire domain can be written as:

$$\int_0^{\eta_{max}} w_1(f_\eta - h) = 0, \tag{3.20}$$

$$\int_0^{\eta_{max}} w_2\left(Sh_\tau + h^2 - fh_\eta + M^2h - h_\eta - k_1(Sh_{\eta\eta\tau} + 2hh_{\eta\eta} - h_\eta^2 - h_{\eta\eta\eta})\right) = 0, \tag{3.21}$$

$$\int_0^{\eta_{max}} w_3\left(S\theta_\tau + 2h\theta - f\theta_\eta - \frac{1}{Pr}\theta_{\eta\eta} - Ech_\eta^2 - M^2Ech^2\right) = 0, \tag{3.22}$$

where w_1, w_2, w_3 are arbitrary test functions and may be viewed as the variation in f, h, θ respectively.

The element free Galerkin model of the equations (3.20)-(3.22) may be obtained dy substituting moving least square approximation for the unknown variables f, h, θ using equations (3.18), (3.19).

$f(\eta,\tau) = \sum_{I=1}^{n} \Phi_I(\eta) f_I(\tau)$, $h(\eta,\tau) = \sum_{I=1}^{n} \Phi_I(\eta) h_I(\tau)$, $\theta(\eta,\tau) = \sum_{I=1}^{n} \Phi_I(\eta)\theta_I(\tau)$.

After simplifying the above system, we arrive at following system of equations:

$$\int_0^{\eta_{max}} w_1(f_\eta - h) = 0 \tag{3.23}$$

$$\begin{aligned}\int_0^{\eta_{max}} & w_2(Sh_\tau + h^2 - fh_\eta + M^2h - h_\eta + h_\eta^2)d\eta + k_1S\int_0^{\eta_{max}} (w_2)_\eta h_{\eta\tau} d\eta \\ & +2k_1\int_0^{\eta_{max}} (w_2)_\eta hh_\eta d\eta - k_1\int_0^{\eta_{max}} (w_2)_\eta h_{\eta\eta} d\eta - (w_2k_1Sh_{\eta\tau})_0^{\eta_{max}} \\ & -(w_2k_12hh_\eta)_0^{\eta_{max}} + (w_2k_1h_{\eta\eta})_0^{\eta_{max}}\end{aligned} \tag{3.24}$$

$$\begin{aligned}\int_0^{\eta_{max}} & w_3(S\theta_\tau + 2h\theta - f\theta_\eta - Ech_\eta^2 - M^2Ech^2 d\eta + \int_0^{\eta_{max}} (w_3)_\eta \frac{1}{Pr}\theta_\eta d\eta \\ & -(w_3\frac{1}{Pr}\theta_\eta)_0^{\eta_{max}}\end{aligned} \tag{3.25}$$

Now, using essential boundary conditions on w_1, w_2, w_3 as homogeneous conditions, equation (3.23), (3.24) and (3.25) become

$$\int_0^{\eta_{max}} w_1(f_\eta - h) = 0 \tag{3.26}$$

$$\int_0^{\eta_{max}} w_2(Sh_\tau + h^2 - fh_\eta + M^2h - h_\eta + h_\eta^2)d\eta + k_1 S \int_0^{\eta_{max}} (w_2)_\eta h_{\eta\tau} d\eta$$
$$+2k_1 \int_0^{\eta_{max}} (w_2)_\eta h h_\eta d\eta - k_1 \int_0^{\eta_{max}} (w_2)_\eta h_{\eta\eta} d\eta \quad (3.27)$$
$$\int_0^{\eta_{max}} w_3(S\theta_\tau + 2h\theta - f\theta_\eta - Ech_\eta^2 - M^2Ech^2)d\eta + \int_0^{\eta_{max}} (w_3)_\eta \frac{1}{Pr}\theta_\eta d\eta \quad (3.28)$$

Next, the equations (3.26) to (3.28) are linearized by incorporating function $\overline{f}$, $\overline{\theta}$, $\overline{h}$ where

$$\overline{f} = \sum_{I=1}^{n} \overline{f}_I \Phi_I, \quad \overline{h} = \sum_{I=1}^{n} \overline{h_I}\Phi_I, \quad \overline{\theta} = \sum_{I=1}^{n} \overline{\theta_I}\Phi_I \quad (3.29)$$

Now, in order to enforce essential boundary conditions, the penalty method is applied on above equations one by one as follows:

From equation (3.26), we get

$$\int_0^{\eta_{max}} w_1(f_\eta - h)d\eta + \overline{\alpha} w_1(f - f(0))|_{\eta=0} = 0$$
$$\int_0^{\eta_{max}} \Phi_I \left(\sum_{J=1}^{n} \frac{\partial \Phi_J}{\partial \eta} f_J - \sum_{J=1}^{n} \Phi_J h_J \right) d\eta + \overline{\alpha}\Phi_I \left(\sum_{J=1}^{n} \Phi_J f_J - f(0) \right) |_{\eta=0} = 0$$
$$\int_0^{\eta_{max}} \left(\Phi_I \frac{\partial \Phi_J}{\partial \eta} + \overline{\alpha}\Phi_I\Phi_J|_{\eta=0} \right) f_J d\eta - \int_0^{\eta_{max}} \Phi_I \Phi_J h_J d\eta = \overline{\alpha}\Phi_I f(0)|_{\eta=0} \quad (3.30)$$

From equation (3.27), we get

$$\int_0^{\eta_{max}} w_2(Sh_\tau + \overline{h}h - \overline{f}h_\eta + M^2h - h_\eta + \overline{h_\eta}h_\eta)d\eta + k_1 \int_0^{\eta_{max}} S(w_2)_\eta h_{\eta\tau} d\eta$$
$$k_1 \int_0^{\eta_{max}} (2(w_2)_\eta h h_\eta - (w_2)_\eta h_{\eta\eta})\, d\eta + \overline{\alpha} w_2(h - h(0))|_{\eta=0} + \overline{\alpha} w_2(h - h(\infty))|_{\eta=\infty}$$
$$\int_0^{\eta_{max}} \Bigg(\Phi_I S \sum_{J=1}^{n} \Phi_J \dot{h_J} + \overline{h}\Phi_I \sum_{J=1}^{n} \Phi_J h_J - \overline{f}\Phi_I \sum_{J=1}^{n} \frac{\partial \Phi_J}{\partial \eta} h_J + M^2 \Phi_I \sum_{J=1}^{n} \Phi_J h_J$$
$$-\Phi_I \sum_{J=1}^{n} \frac{\partial \Phi_J}{\partial \eta} h_J + k_1 \Phi_I \frac{\partial \overline{h}}{\partial \eta} \sum_{J=1}^{n} \frac{\partial \Phi_J}{\partial \eta} h_J \Bigg) d\eta + k_1 \sum_{J=1}^{n} \int_0^{\eta_{max}} \Bigg(S \frac{\partial \Phi_I}{\partial \eta}\frac{\partial \Phi_J}{\partial \eta} \dot{h}$$
$$+2\overline{h}\frac{\partial \Phi_I}{\partial \eta}\frac{\partial \Phi_J}{\partial \eta} h_J - \frac{\partial \Phi_I}{\partial \eta}\frac{\partial^2 \Phi_J}{\partial \eta^2} \Bigg) d\eta + \overline{\alpha}\Phi_I \left(\sum_{J=1}^{n} \Phi_J h_J - h(0) \right) |_{\eta=0}$$
$$+\overline{\alpha}\Phi_I \left(\sum_{J=1}^{n} \Phi_J h_J - h(\infty) \right) |_{\eta=\infty}$$
$$(3.31)$$

$$\int_0^{\eta_{max}} \left(\overline{h}\Phi_I\Phi_J - \overline{f}\Phi_I\frac{\partial \Phi_J}{\partial \eta} + M^2\Phi_I\Phi_J - \Phi_I\frac{\partial \Phi_J}{\partial \eta} + k_1\Phi_I\frac{\partial \overline{h}}{\partial \eta}\frac{\partial \Phi_J}{\partial \eta} + 2k_1\overline{h}\frac{\partial \Phi_I}{\partial \eta}\frac{\partial \Phi_J}{\partial \eta}\right.$$
$$\left. -k_1\frac{\partial \Phi_I}{\partial \eta}\frac{\partial^2 \Phi_J}{\partial \eta^2} + \overline{\alpha}\Phi_I\Phi_J|_{\eta=0} + \overline{\alpha}\Phi_I\Phi_J|_{\eta=\infty}\right) h_J d\eta + \int_0^{\eta_{max}} \left(S\Phi_I\Phi_J\right.$$
$$\left. +k_1 S\frac{\partial \Phi_I}{\partial \eta}\frac{\partial \Phi_J}{\partial \eta}\right)\dot{h}d\eta = \overline{\alpha}\Phi_I h(0)|_{\eta=0} + \overline{\alpha}\Phi_I h(\infty)|_{\eta=\infty} \qquad (3.32)$$

From equation (3.28), we get

$$\int_0^{\eta_{max}} w_3(S\theta_\tau + 2\overline{h}\theta - \overline{f}\theta_\eta - Ec\overline{h_\eta}h_\eta - M^2Ec\overline{h}h)d\eta + \int_0^{\eta_{max}} (w_3)_\eta\frac{1}{Pr}\theta_\eta d\eta$$
$$+\overline{\alpha}w_3(\theta - \theta(0))|_{\eta=0} + \overline{\alpha}w_3(\theta - \theta(\infty))|_{\eta=\infty}$$

$$\int_0^{\eta_{max}} \left(S\Phi_I\sum_{J=1}^{n}\Phi_J\dot{\theta} + 2\overline{h}\Phi_I\sum_{J=1}^{n}\Phi_J\theta_J - \overline{f}\Phi_I\sum_{J=1}^{n}\frac{\partial \Phi_J}{\partial \eta}\theta_J - Ec\Phi_I\frac{\partial \overline{h}}{\partial \eta}\sum_{J=1}^{n}\frac{\partial \Phi_J}{\partial \eta}h_J\right.$$
$$\left. -M^2Ec\Phi_I\overline{h}\sum_{J=1}^{n}\Phi_J h_J\right)d\eta + \int_0^{\eta_{max}} \frac{1}{Pr}\frac{\partial \Phi_I}{\partial \eta}\sum_{J=1}^{n}\frac{\partial \Phi_J}{\partial \eta}\theta_J d\eta$$
$$+\overline{\alpha}\Phi_I\left(\sum_{J=1}^{n}\Phi_J\theta_J - \theta(0)\right)|_{\eta=0} + \overline{\alpha}\Phi_I\left(\sum_{J=1}^{n}\Phi_J\theta_J - \theta(\infty)\right)|_{\eta=\infty}$$

$$\int_0^{\eta_{max}} \left(-Ec\Phi_I\frac{\partial \overline{h}}{\partial \eta}\frac{\partial \Phi_J}{\partial \eta} - M^2Ec\Phi_I\overline{h}\Phi_J\right)h_J d\eta + \int_0^{\eta_{max}} \left(\frac{1}{Pr}\frac{\partial \Phi_I}{\partial \eta}\frac{\partial \Phi_J}{\partial \eta} + 2\overline{h}\Phi_I\Phi_J\right.$$
$$\left. -\Phi_I\overline{f}\frac{\partial \Phi_J}{\partial \eta} + \overline{\alpha}\Phi_I\Phi_J|_{\eta=0} + \overline{\alpha}\Phi_I\Phi_J|_{\eta=\infty}\right)\theta_J d\eta + \int_0^{\eta_{max}} S\Phi_I\Phi_J\dot{\theta}d\eta$$
$$= \overline{\alpha}\Phi_I\theta(0)|_{\eta=0} + \overline{\alpha}\Phi_I\theta(\infty)|_{\eta=\infty} \qquad (3.33)$$

where $f(0), h(0), h(\infty), \theta(0), \theta(\infty)$ are given in equation (3.14). $\overline{\alpha}$ is the penalty parameter and in the present work, it is chosen as 10^6.

In the matrix form, equations (3.30)-(3.32) can be written as follows:

$$[K]\{\overline{H}\} + [M]\{\overline{\overline{H}}\} = \{F\} \qquad (3.34)$$

where

$$[K] = \begin{bmatrix} K_{11} & K_{12} & K_{13} \\ K_{21} & K_{22} & K_{23} \\ K_{31} & K_{32} & K_{33} \end{bmatrix}, \quad [M] = \begin{bmatrix} 0 & 0 & 0 \\ 0 & M_2 & 0 \\ 0 & 0 & M_3 \end{bmatrix}, \quad \{\overline{H}\} = \begin{bmatrix} \{f\} \\ \{h\} \\ \{\theta\} \end{bmatrix}$$

$$\{\overline{\overline{H}}\} = \begin{bmatrix} \{\dot{f}\} \\ \{\dot{h}\} \\ \{\dot{\theta}\} \end{bmatrix} \quad \{F\} = \begin{bmatrix} \{F_1\} \\ \{F_2\} \\ \{F_3\} \end{bmatrix}$$

and the entries of the matrix $[K]$ are given by

$$(K_{11})_{IJ} = \int_0^{\eta_{max}} \Phi_I \frac{\partial \Phi_J}{\partial \eta} d\eta + \overline{\alpha}\Phi_I\Phi_J|_{\eta=0},$$

$$(K_{12})_{IJ} = -\int_0^{\eta_{max}} \Phi_I\Phi_J d\eta,$$

$$(K_{13})_{IJ} = 0,$$

$$(K_{21})_{IJ} = 0,$$

$$(K_{22})_{IJ} = \int_0^{\eta_{max}} \left(\overline{h}\Phi_I\Phi_J - \overline{f}\Phi_I\frac{\partial \Phi_J}{\partial \eta} + M^2\Phi_I\Phi_J - \Phi_I\frac{\partial \Phi_J}{\partial \eta} + k_1\Phi_I\frac{\partial \overline{h}}{\partial \eta}\frac{\partial \Phi_J}{\partial \eta} + 2k_1\overline{h}\frac{\partial \Phi_I}{\partial \eta}\frac{\partial \Phi_J}{\partial \eta} - k_1\frac{\partial \Phi_I}{\partial \eta}\frac{\partial^2 \Phi_J}{\partial \eta^2}\right) d\eta + \overline{\alpha}\Phi_I\Phi_J|_{\eta=0} + \overline{\alpha}\Phi_I\Phi_J|_{\eta=\infty}$$

$$(K_{23})_{IJ} = 0,$$

$$(K_{31})_{IJ} = 0,$$

$$(K_{32})_{IJ} = \int_0^{\eta_{max}} \left(-Ec\Phi_I\frac{\partial \overline{h}}{\partial \eta}\frac{\partial \Phi_J}{\partial \eta} - M^2Ec\Phi_I\overline{h}\Phi_J\right) d\eta,$$

$$(K_{33})_{IJ} = \int_0^{\eta_{max}} \left(\frac{1}{Pr}\frac{\partial \Phi_I}{\partial \eta}\frac{\partial \Phi_J}{\partial \eta} + 2\overline{h}\Phi_I\Phi_J - \Phi_I\overline{f}\frac{\partial \Phi_J}{\partial \eta}\right) d\eta + \overline{\alpha}\Phi_I\Phi_J|_{\eta=0} + \overline{\alpha}\Phi_I\Phi_J|_{\eta=\infty},$$

$$(M_{11})_{IJ} = 0,$$

$$(M_{12})_{IJ} = 0,$$

$$(M_{13})_{IJ} = 0,$$

$$(M_{21})_{IJ} = 0,$$

$$(M_{22})_{IJ} = \int_0^{\eta_{max}} \left(S\Phi_I\Phi_J + k_1S\frac{\partial \Phi_I}{\partial \eta}\frac{\partial \Phi_J}{\partial \eta}\right) d\eta,$$

$$(M_{23})_{IJ} = 0,$$

$$(M_{31})_{IJ} = 0,$$

$$(M_{32})_{IJ} = 0,$$

$$(M_{33})_{IJ} = \int_0^{\eta_{max}} S\Phi_I\Phi_J d\eta,$$

$$(F_1)_I = f(0)\overline{\alpha}\Phi_I|_{\eta=0}$$

$$(F_2)_I = h(0)\overline{\alpha}\Phi_I|_{\eta=0} + h(\infty)\overline{\alpha}\Phi_I|_{\eta=\infty}$$

$$(F_3)_I = \theta(0)\overline{\alpha}\Phi_I|_{\eta=0} + \theta(\infty)\overline{\alpha}\Phi_I|_{\eta=\infty}$$

For time integration, Crank-Nicolson scheme is used which is unconditionally stable. Following Crank-Nicolson scheme, equation (3.33) at $(p+1)^{th}$ time step can be written as :

$$[\hat{K}]_{p+1}[\bar{H}]_{p+1} = [\hat{K}]_p[\bar{H}]_p + [F]_{p,p+1}$$

where $[\hat{K}]_{p+1} = [M] + \frac{\triangle t}{2}[K]_{p+1}$, $[\hat{K}]_p = [M] - \frac{\triangle t}{2}[K]_p$ and
$[F]_{p,p+1} = \frac{\triangle t}{2}[\{F\}_p + \{F\}_{p+1}]$
The whole domain Ω is discretized with uniformly distributed 101 nodes. Four point Gauss quadrature formula has been used to calculate the integral values. At each node three functions f, h, θ are to be evaluated, hence after assembly, we obtain a non-linear systems of equations of order 303x303, as given in (24). Owing to the nonlinearity of the system an iterative scheme has been used to solve it with an initial guess. The system of equations is linearized by incorporating known functions $\overline{f}, \overline{h}, \overline{\theta}$, which is solved using Gauss elimination method. This gives a new set of values of unknowns f, h, θ and the process continues till the absolute difference of two successive iterate value of unknowns is less than the accuracy 0.0005.
It has been observed that in the same domain, the accuracy is not affected even if the numbers of nodes are increased, else it increases the computational time only.

3.2 Results and discussion

In order to obtain some physical insight into present simulation, numerical computations are carried out for various values of the parameters that describe the flow characteristics and the results are reported in terms of graphs.

Figure 1 shows the time series of the velocity field $h(= f_\eta)$ at the four different distance from the surface of the oscillatory sheet with fixed values of $S = 1$, $M = 2$, $Pr = 5.0$, $k1 = 0.2$, $Ec = 0.2$. It is observed that the amplitude of the flow near the oscillatory surface is greater as compared to that far away from the surface. As the distance increase from the surface, the amplitude of the flow motion is decreased and almost vanishes (approached to zero) for larger distance from the sheet.

Figure 2 depicts the effect of viscoelastic parameter $k1$ on the time series $\tau\epsilon[0,4\pi]$ of the velocity field $h(=f_\eta)$ at a fixed distance $\eta = 0.2$ from the surface. An increment in the amplitude of the flow motion is observed with the increase of the non-Newtonian viscoelastic parameter $k1$ due to increased effective viscosity.

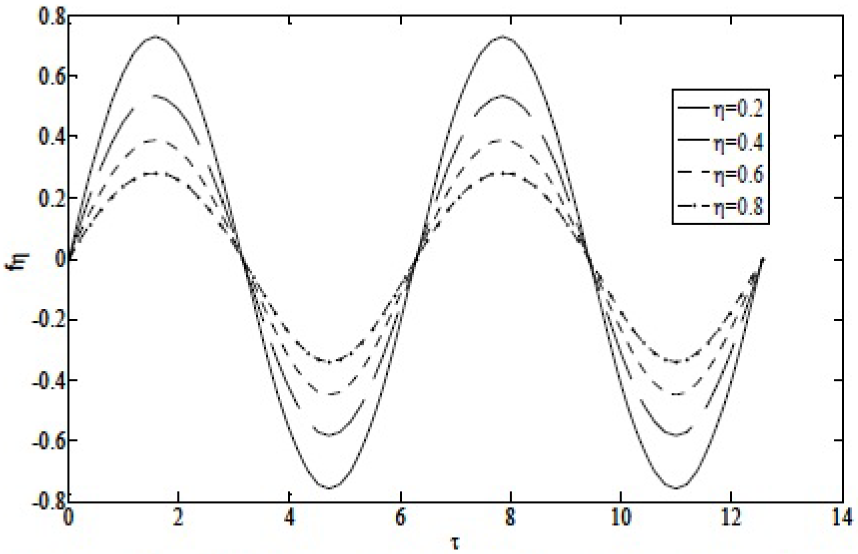

Fig. 1 $f_\eta(\eta,\tau)$ with S=1.0, M=2.0, k_1=0.4, Pr=5.0 and Ec=0.2

In Figure 3 the effect parameter S (ratio of oscillation frequency of sheet to its stretching rate) on the time series $\tau\epsilon[0,4\pi]$ of the velocity field is depicted. It is observed that with the increase of S the amplitude of the flow increases slightly.

Figure 4 depicts velocity profile f_η for the different values of the magnetic parameter M keeping fixed values $S = 1.0$, $k1 = 0.2$, $Pr = 5.0$, $Ec = 0.2$. As expected, the magnetic field in an electrically conduction flow acts as a drag-like force called the Lorentz force. This type of resistive force tends to slow down the motion of the fluid in the boundary layer i.e decelerates the flow. Hence, the amplitude of the flow decreases with the increase of the magnetic parameter M. Due to deceleration of the flow, temperature of the fluid is increased.

Figure 5 reveals the relative influence of magnetic field in temperature $\theta(\eta,\tau)$.

Figure 6 illustrates the effect of Prandtl number Pr on the temperature profile $\theta(\eta,\tau)$

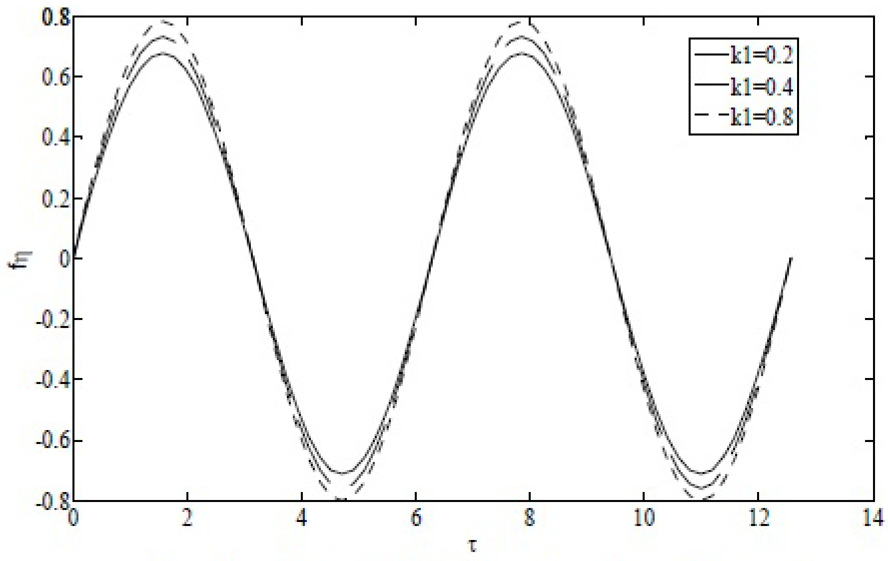

Fig 2 $f_\eta(\eta,\tau)$ with S=1.0, M=2.0, Pr=5.0 and Ec=0.2

at $\tau = \pi/4$. It is observed that the effect of increasing Prandtl number Pr is to decrease, temperature throughout the boundary layer, which results in decrease of the thermal boundary layer thickness. The increase of Prandtl number means slow rate of thermal diffusion.

Figure 7 depicts that the effect of increasing the values of local Eckert number Ec is to increase temperature distribution in the flow region. This behavior of temperature enhancement occurs as heat energy is stored in the fluid due to frictional heating.

Table 3.1: Comparison of results for the Nusselt number $-\theta_n(0)$ with $k_1 = 0.0$, $M = 0.0$, $S = 0.0$, $Ec = 0.0$ and various values of Pr with Chen and Grubka and Bobba.

Pr	$Chen$[7]	$Grubka\ \ and\ \ Bobba$[12]	$Present\ \ results$
1.0	1.33334	1.3333	1.3333
2.0	-	-	1.9876
3.0	2.50972	2.5097	2.5095
5	-	-	3.6577
10.0	4.79686	4.7969	4.7968

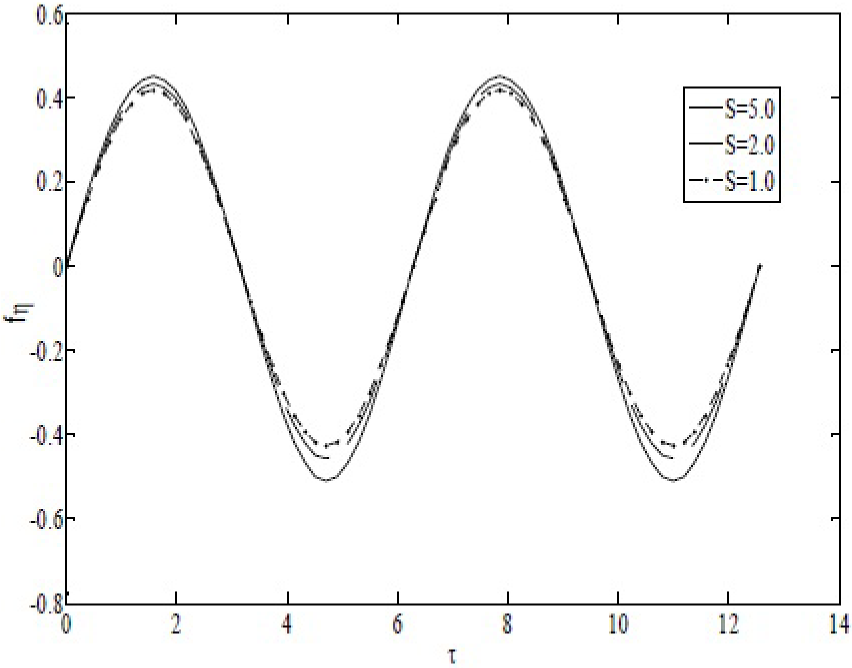

Fig. 3 $f_\eta(\eta, \tau)$ with k_1=0.2, M=2.0, Pr=5.0 and Ec=0.2, $\eta = 0.4$

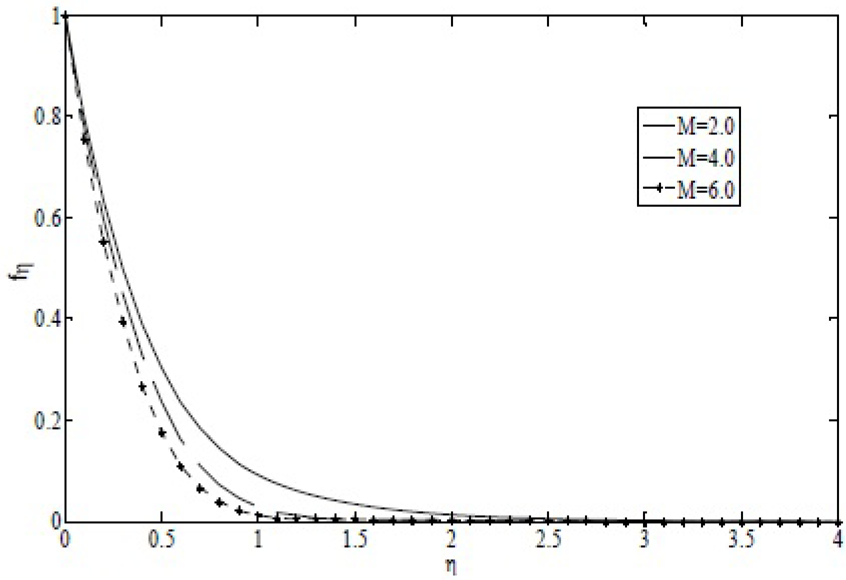

Fig. 4 $f_\eta(\eta, \tau)$ with k_1=0.2, S=1.0, Pr=5.0, Ec=0.2, $\tau = \pi / 2$

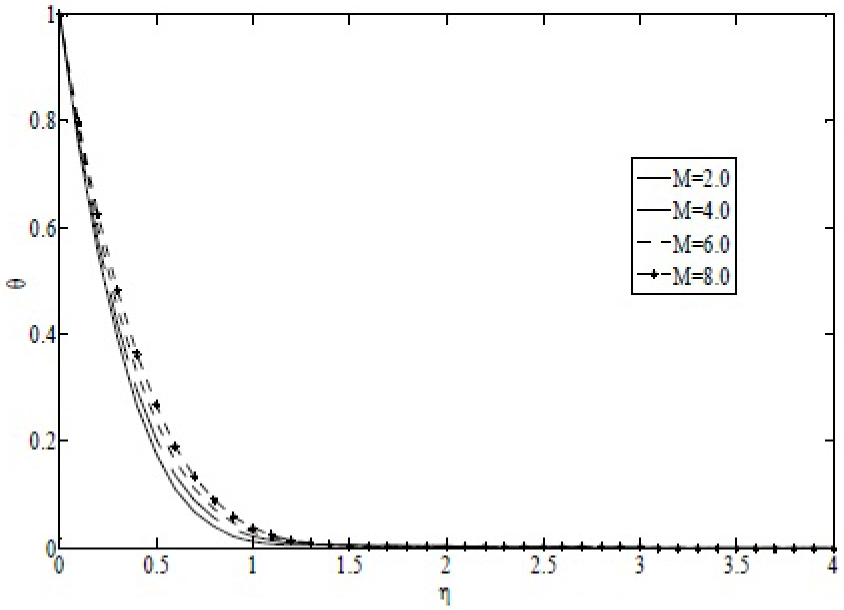

Fig. 5 $\theta(\eta, \tau)$ with k_1=0.2, S=1.0, Pr=5.0, Ec=0.2, $\tau = \pi / 2$

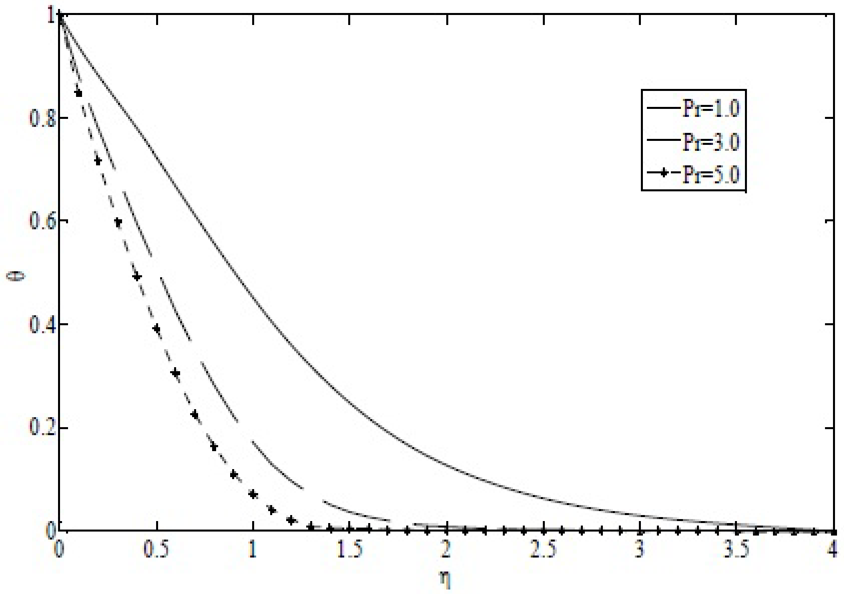

Fig. 6 $\theta(\eta, \tau)$ with k_1=0.2, S=1.0, M=2.0, Ec=0.2, $\tau = \pi / 4$

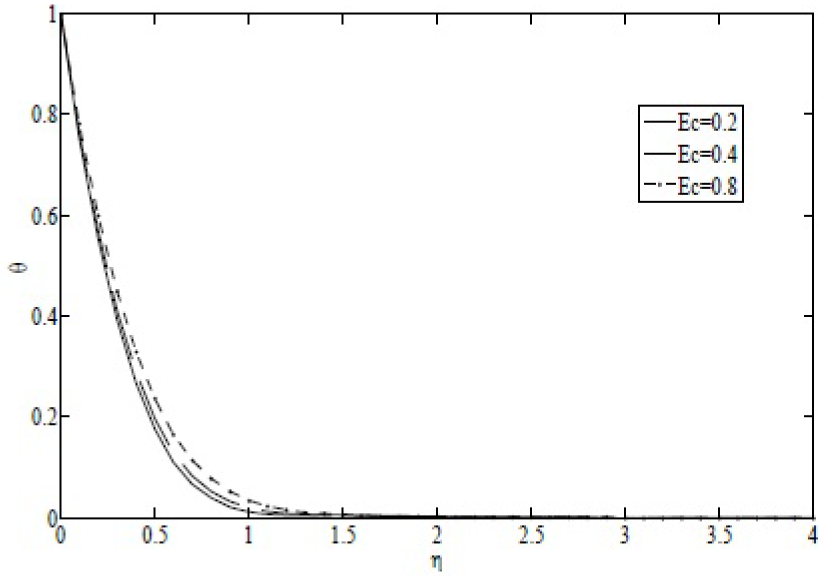

Fig. 7 $\theta(\eta, \tau)$ with k_1=0.2, S=1.0, Pr=5.0, M=2.0, $\tau = \pi / 2$

References

[1] R.S. Agarwal, R. Bhargava, A.V.S. Balaji, Int. J. Eng. Sci., 1989; 27, 1421-1428.

[2] Z. Abbas, Y. Wang, T. Hayat, M. Oberklack, Hydromagnetic flow in a viscoelastic fluid due to the oscillatory stretching surface, 2008; 43, 783-793.

[3] T. Belytscho, L. Gu, Y.Y. Lu, Fracture and crack growth by element free Galerkin method, 1994; 2, 519-534.

[4] T. Belytscho, L. Gu, Y.Y. Lu, M. Tabbara, int. J. Soilds struct., 1995; 32, 2547-2570.

[5] R. Bhargava, O.A. Beg, S. Sharma, J. Zueco, Commun. nonlinear science numer. simulation, 2010; 15, 1210-1223.

[6] V. Cingoski, N. Miyamoto, H. Yamashita, IEEE trans. Magnetics, 1998; 34, 3236-3239.

[7] C.H. Chen, Laminar mixed convention adjacent to vertical continuously stretching sheets, 1998; 33, 471-476.

[8] J.E. Dunn, K.R. Rajagopal, Fluids of differential type-critical review and thermodynamic analysis, 1995; 33, 689-729.

[9] A.C. Eringer, Int. J. Eng. Sci., 1964; 2, 205-217.

[10] A.C. Eringer, J. Math. Mech., 1966; 16, 1-16.

[11] R.L. Fosdick, K.R. Rajagopal, Thermodynamics and stability of fluids of third grade, 1980; 369, 351-377.

[12] L.J. Grubka and K.M. Bobba, Heat transfer characteristic of a continuous stretching surface with variable temperature, 1985; 107,248-250.

[13] R.S. Gupta, Elements of Numerical Analysis, Macmillan, 2008.

[14] A. Ishak, R. Nazar, I. Por. Heat Mass Transfer, 2008; 44, 921-927.

[15] G.R. Liu, Mesh free method-Moving beyond the Finite Element method, CRC Press, 2003.

[16] J.B. Laurindo, M. Part., Chem. Eng. Sci., 1998; 53, 2257-2269.

[17] J.N. Reddy, An Introduction to Finite Element Methods, McGraw-Hill, New York, 2006.

[18] M.D. Raisinghania, Ordinary and Partial Differential Equations, S. Chand, 2008.

[19] A. Singh, I.V. Singh, R. Parkash, Numerical analysis of fluid squeezed between two parallel plates by meshless method, 2007; 36, 1460-1480.

[20] I.V. Singh, K. Sandeep, R. Parkash, Numer. heat transfer, 2003; 44, 73-84.

[21] M.A. Seddeek, S.N. Odda, M.Y. Akl, M.S. Abdelmeguid, Comput. master. sci., 2009; 45, 423-428.

[22] H. Wu, F. Jintu, D. Ning. J. Appl. Polymer Sci., 2007; 106, 576-583.

[23] R. Sharma, R. Bhargava and P. Bhargava, A numerical solution of unsteady MHD convection heat and mass transfer past a semi-infinite vertical porous moving plate using element free Galerkin method, 2010; 3, 397-407.

[24] R. Sharma, Appl. Math. Comput., 2012; 219, 976-987.

[25] R. Sharma, R. Bhargava, I.V. Singh, Appl. Math. Comput.,2010; 217, 303-321.

[26] S.L. Ross, Differential Equation, John Wiley and Sons, 2004.

[27] S. Kenawy, M. Awaad, S. Naga, H. Windsheimer, P. Greil., Int . J. Appl. Ceramic Technol., 2008; 5,618-623.

[28] S. Mukhopadhyay, I.C¿ Mondal, R.S.R Gorla, Heat Mass Transf., 2012; 48, 915-921.

[29] S. Singh, R. Bhargava, Element free Galerkin simulation of micropolar squeeze film flow of a biological lubricant, 2012; 3, 149-152.

[30] T. Zhu, S.N. Atluri, Comput. Mech., 1998, 21, 211-222.

[31] V.M. Soundalgekar, S.K. Gupta, Free convection effects on an oscillatory flow of viscous, incompressible fluid past a steadily moving vertical plate with constant function, 1975; 18, 1083-1093.

[32] Y.Y. Lu, T. Belytschko, M. Tabbara, Comput. Math. Appl. Mech. Eng., 1995; 126, 131-153.